Advanced Detectors for Nuclear, High Energy and Astroparticle Physics
15-17 February 2017
Bose Institute, Kolkata, India

Silicon Sensors in Experimental High Energy Physics Experiments

Ashutosh Bhardwaj
Department of Physics & Astrophysics
University of Delhi - India

Outline

- Silicon Detectors: Historical Perspective
- Highlights
- Basics of Si detectors & Principle of operation
- Radiation Damage Mechanism
- HPK Campaign & DU’s Involvement
- Radiation Damage Modeling
- India in CMS Outer Tracker Phase II upgrade
- Detector Development at DU
- Some Novel Detector Designs
- Summary

Historical Perspective

- 1951: First detectors with Germanium pn-Diodes (McKay)
- 1960: Working samples of p-i-n Detectors for α & β Spectroscopy (E. M. Pell)
- 1964: Use of Si detectors in experimental Nuclear Physics (G. T. Ewan & A. J. Tavendale)
- 1980: Fixed target experiment with a planar diode (J. Kemmer)
- 1980-86: NA11 & NA32 experiment at CERN to measure charm meson lifetimes
- 1990ies (Europe): LEP Detectors (e.g. DELPHI)
- 1990ies & later (US): CDF & D0 at Tevatron, Fermilab
- Today: All Detectors at LHC with upto 200 m^2 active area (CMS)

Historical Perspective

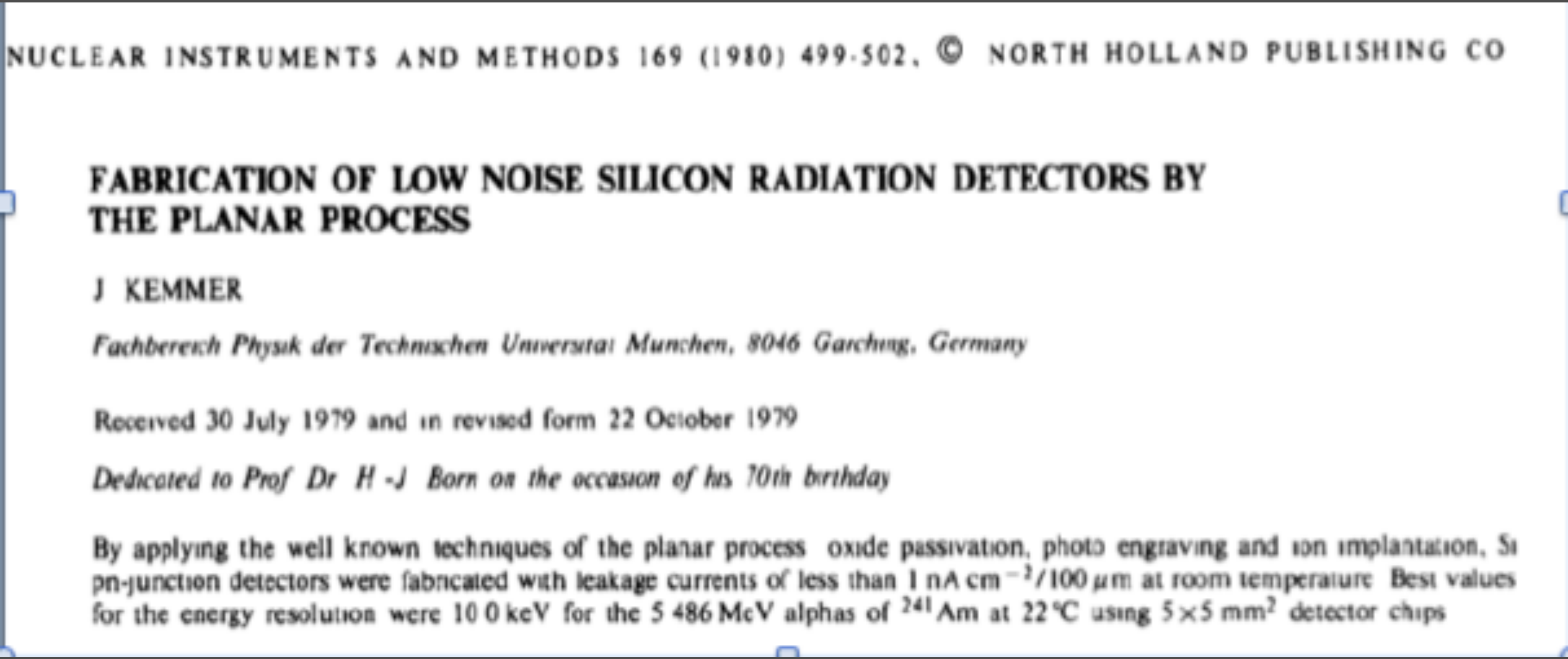

NUCLEAR INSTRUMENTS AND METHODS 169 (1980) 499-502, © NORTH HOLLAND PUBLISHING CO

FABRICATION OF LOW NOISE SILICON RADIATION DETECTORS BY THE PLANAR PROCESS

J KEMMER

Fachbereich Physik der Technischen Universitat Munchen, 8046 Garching, Germany

Received 30 July 1979 and in revised form 22 October 1979

Dedicated to Prof Dr H -J Born on the occasion of his 70th birthday

By applying the well known techniques of the planar process oxide passivation, photo engraving and ion implantation, Si pn-junction detectors were fabricated with leakage currents of less than 1 nA cm^{-2}/100 μm at room temperature Best values for the energy resolution were 10 0 keV for the 5 486 MeV alphas of ^{241}Am at 22 °C using 5×5 mm^2 detector chips

Why wasn't silicon used earlier?

- Needed micro-lithography technology ⇒ cost
- Small signal size (needed low noise amplifiers)
- Needed read-out electronics miniaturization (transistors, ICs)

Historical Perspective

NA11 @ CERN : fixed target experiment ~ 1980

First proof of principle to use a position sensitive silicon detector in HEP experiment

- Aim: measure lifetime of charm quarks (decay length 30 μm) ⇒ spatial resolution better 10μm required

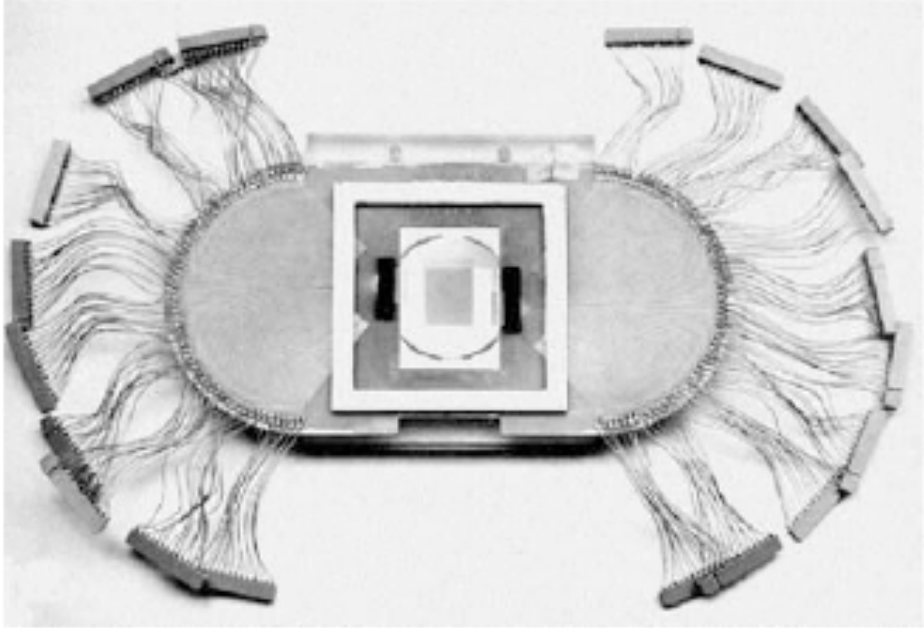

NA11 Detector:

- 1200 diode strips on 2436mm^2 active area
- Resolution of 4.5 μm
- 250-500 μm thick bulk material

Historical Perspective

NA11 @ CERN : fixed target experiment ~ 1980

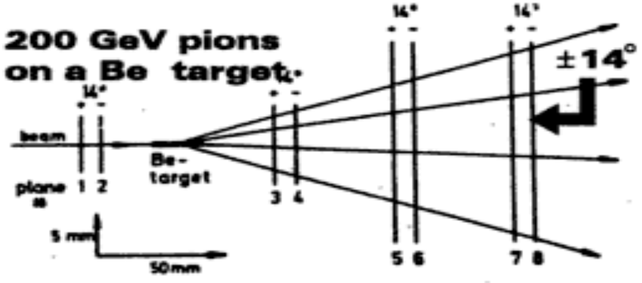

1983

8 layers of single sided Si detectors
strip pitch: 20 µm
readout pitch: 60 µm
spatial resolution: 5 µm

FIRST SILICON VERTEX DETECTOR

CONSTRUCTED TO MEASURE CHARM LIFETIMES

NA 11 → NA 32 → many more

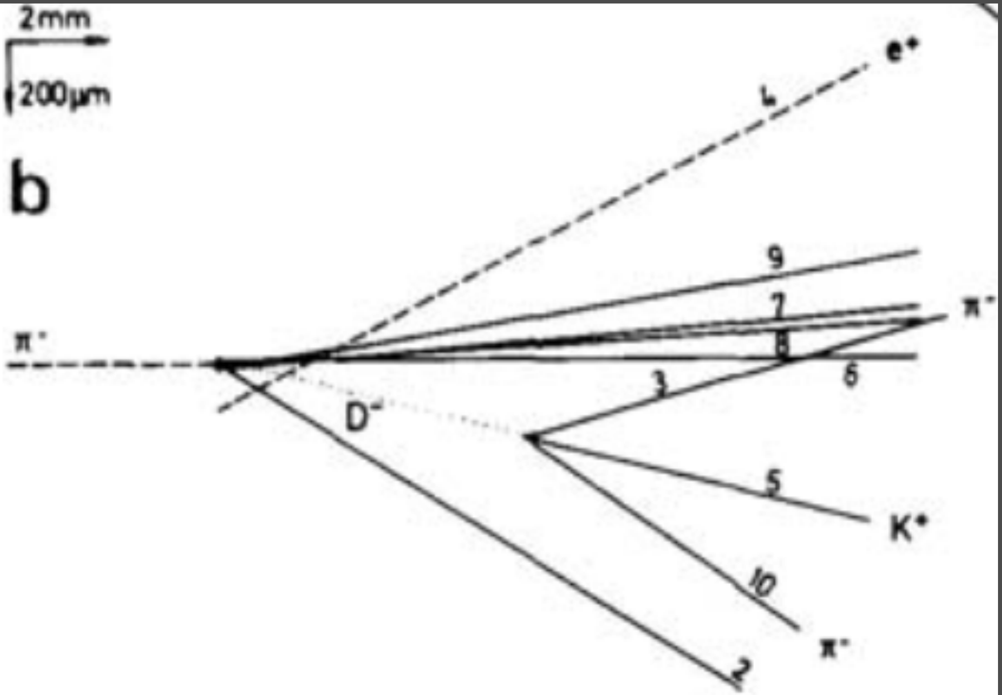

Reconstruction of the production and decay of a $D^- \rightarrow K^+\pi^-\pi^-$

Historical Perspective

John Ellis visioned at a conference in Lake Tahoe, California in 1983, “To proceed with High Energy Particle Physics, one has to tag the flavour of the quarks!”

CDF @ Fermilab : Collider beam Experiment Top Quark Discovery

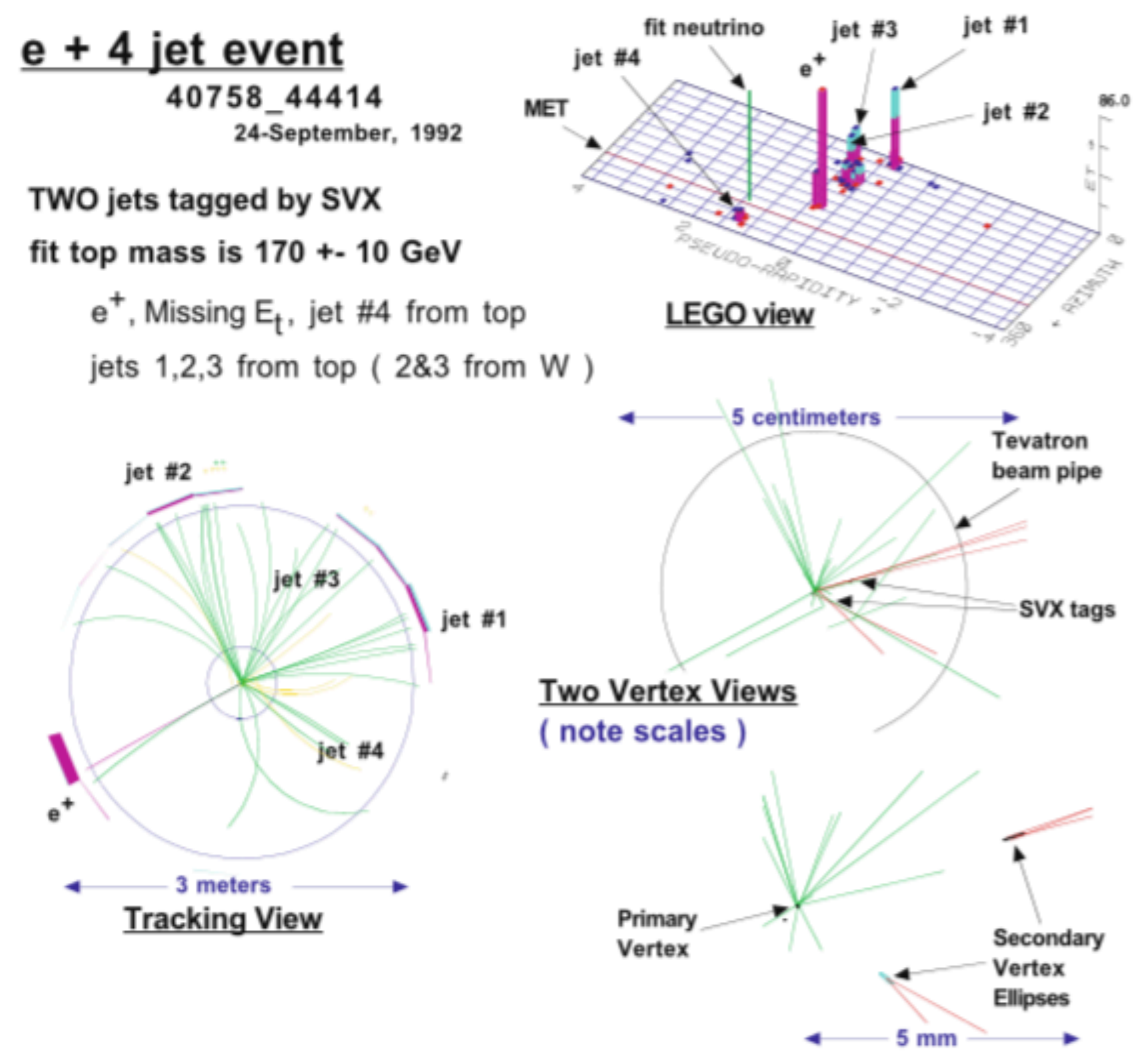

e + 4 jet event

40758_44414

24-September, 1992

TWO jets tagged by SVX

fit top mass is 170 +- 10 GeV

e^+, Missing E_t, jet #4 from top

jets 1,2,3 from top (2&3 from W)

LEGO view

Tracking View

Two Vertex Views

(note scales)

Evolution of Si Detectors in EHEP

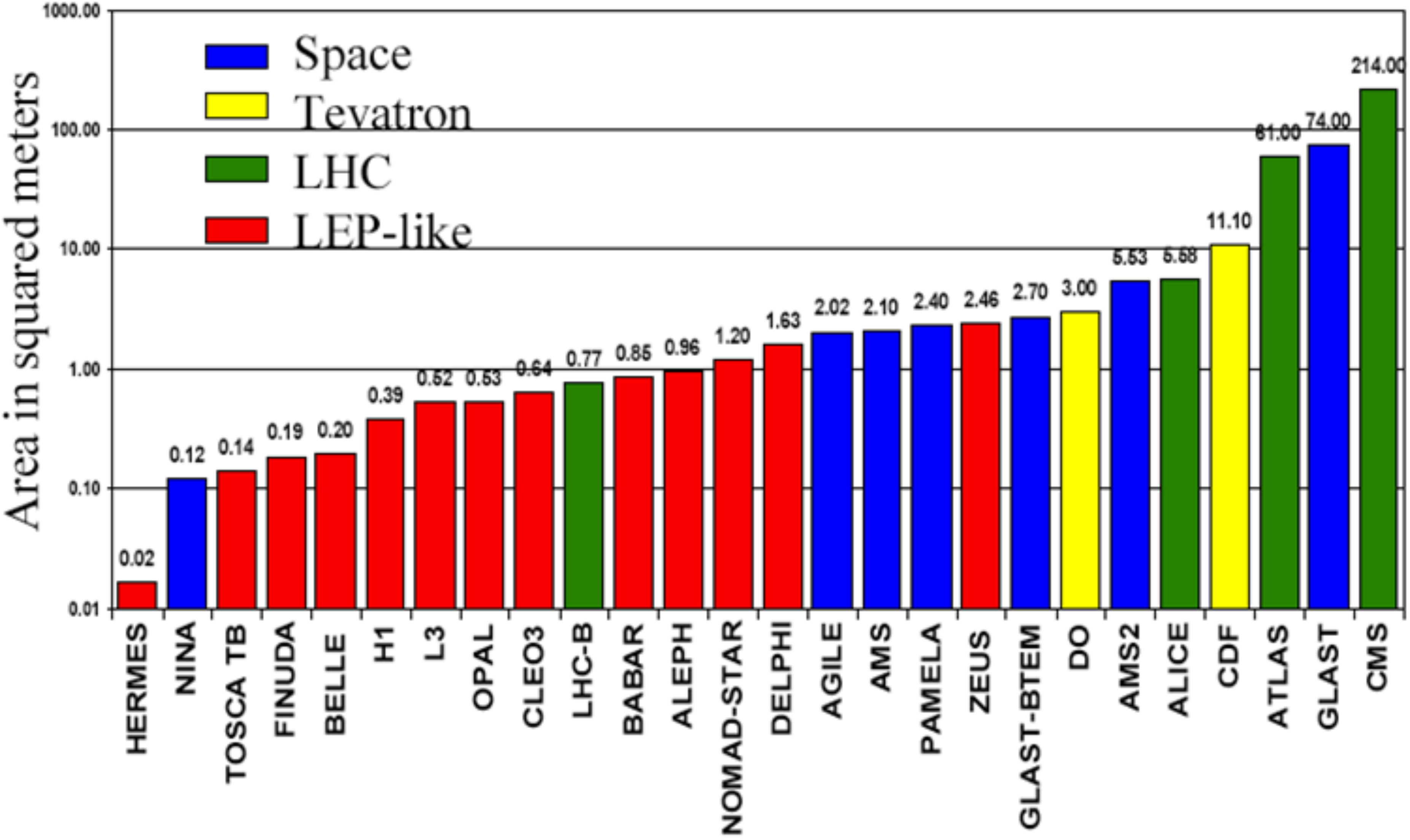

Large Silicon Sytems in EHEP

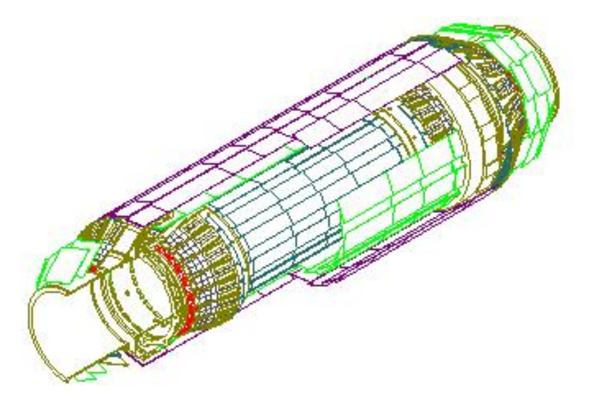

DELPHI (1996)

~ 1.8m^2 silicon area

175 000 readout channels

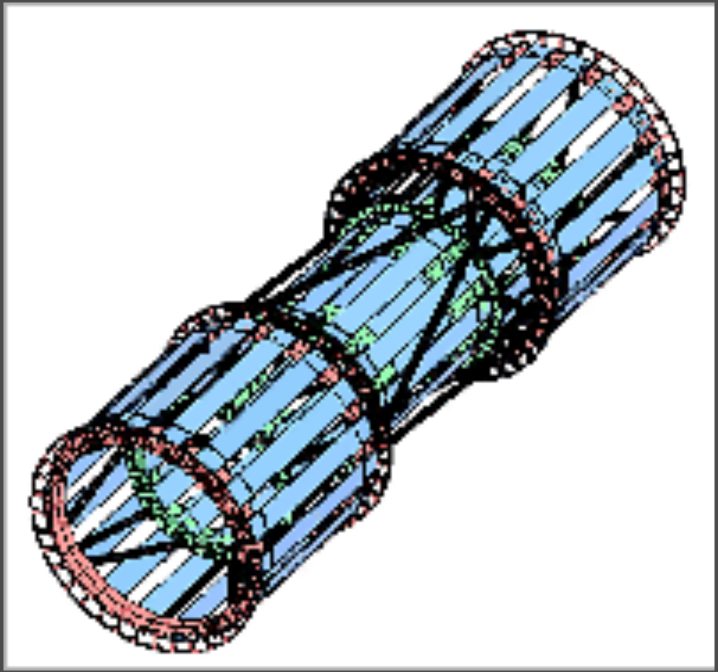

CDF SVX IIa (2001-)

~ 11m^2 silicon area

~ 750 000 readout channels

Large Silicon Sytems in EHEP

CMS Si Tracker (2007)

- ~12,000 modules
- ~ 206 m^2 silicon area
- ~ 25,000 silicon wafers
- ~ 10M readout channels

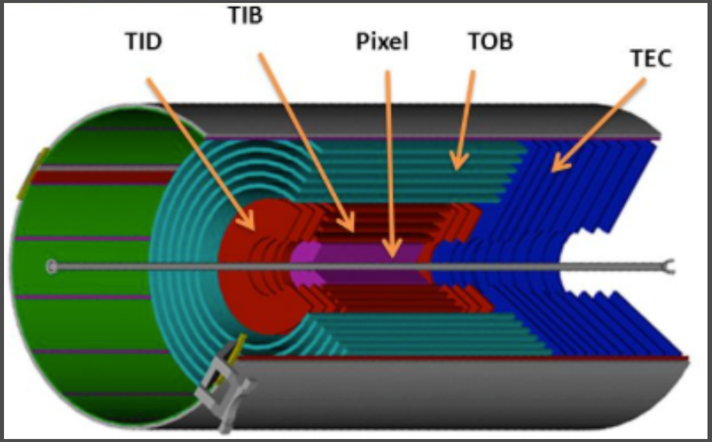

Large Silicon Sytems in EHEP

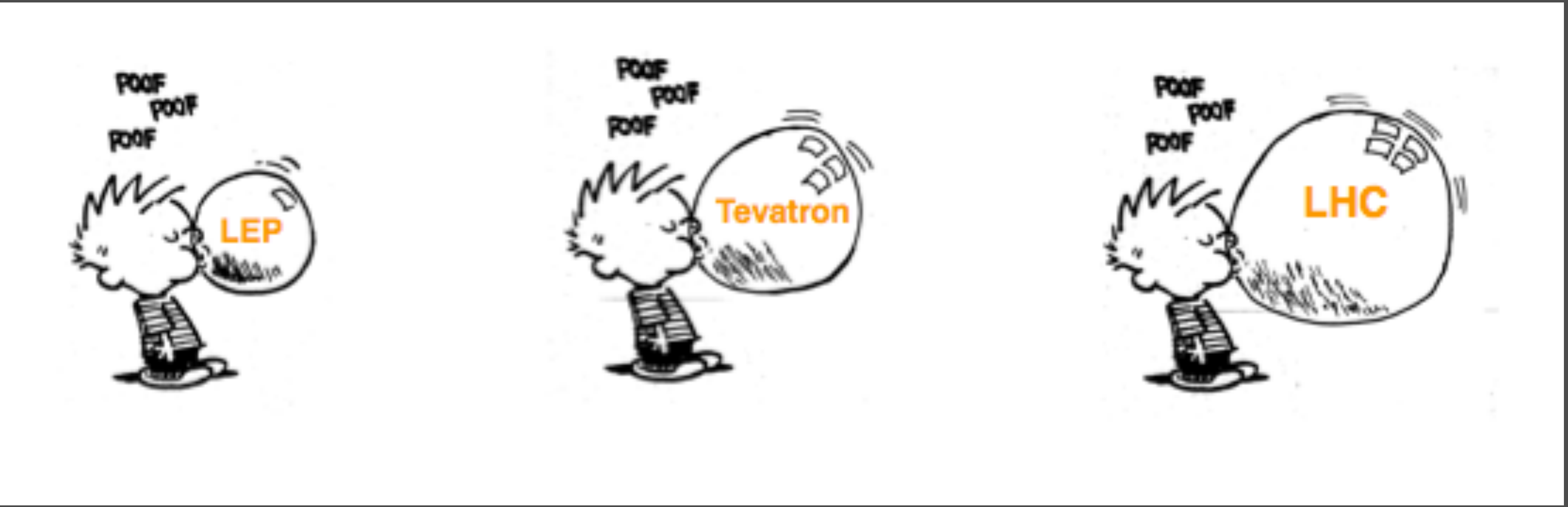

Highlight

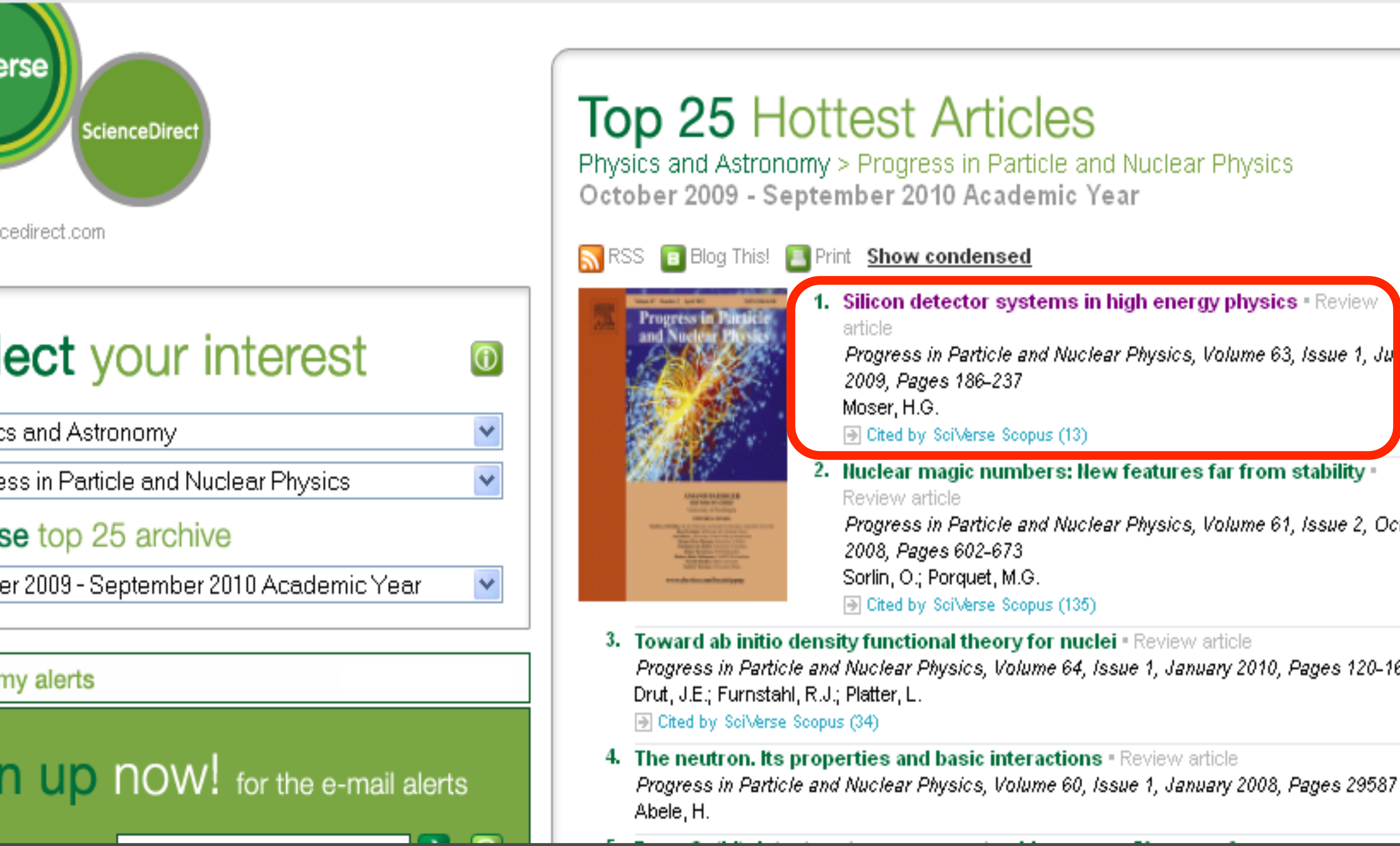

Top 25 Hottest Articles

Physics and Astronomy > Progress in Particle and Nuclear Physics

October 2009 - September 2010 Academic Year

1. **Silicon detector systems in high energy physics** ▪ Review article
   Progress in Particle and Nuclear Physics, Volume 63, Issue 1, Ju
   2009, Pages 186-237
   Moser, H.G.
   Cited by SciVerse Scopus (13)
2. **Nuclear magic numbers: New features far from stability** ▪ Review article
   Progress in Particle and Nuclear Physics, Volume 61, Issue 2, Oc
   2008, Pages 602-673
   Sorlin, O.; Porquet, M.G.
   Cited by SciVerse Scopus (135)
3. **Toward ab initio density functional theory for nuclei** ▪ Review article
   Progress in Particle and Nuclear Physics, Volume 64, Issue 1, January 2010, Pages 120-16
   Drut, J.E.; Furnstahl, R.J.; Platter, L.
   Cited by SciVerse Scopus (34)
4. **The neutron. Its properties and basic interactions** ▪ Review article
   Progress in Particle and Nuclear Physics, Volume 60, Issue 1, January 2008, Pages 29587
   Abele, H.

Some Basic Facts

- By far the most important semiconductor for detector development is silicon
- The discovery of silicon (L. silex: silicis, flint) - *silicium* in French - is generally credited to Berzelius 1824
- Deville in 1854 first prepared crystalline silicon, the second allotropic form of the element
- Silicon is present in the sun and stars
  - principal component of a class of meteorites known as aerolites. It is also a component of tektites, a natural glass of uncertain origin.
- Silicon makes up 25.7% of the earth's crust by weight
  - is the second most abundant element, being exceeded only by oxygen.
- Silicon is not found free in nature, but occurs chiefly as the oxide and as silicates.
  - Sand, quartz, rock crystal, amethyst, agate, flint, jasper, and opal are some of the forms in which the oxide appears. Granite, hornblende, asbestos, feldspar, clay, mica, etc. are but a few of the numerous silicate minerals.

Why Silicon

Silicon has properties which make it especially desirable as a detector material

- Small band gap $E_g = 1.12$ eV ⇒ E(e-h pair) = 3.6 eV (≈ 30 eV for gas detectors) (good signal)
- High specific density 2.33 g/cm^3 ; dE/dx (M.I.P.) ≈ 390 eV/μm ≈ 108 e-h/μm (average)
- High carrier mobility μ_e =1450 cm^2/Vs, μ_h = 450 cm^2/Vs ⇒ fast charge collection (<10 ns)
- Very pure < 1ppm impurities and < 0.1ppb electrical active impurities, long mean free path (good charge collection efficiency)
- low dark current: Can be operated in air and at room temperature
- low Z (low multiple scattering)
- Rigidity of silicon allows thin self supporting structures
- Very well developed technology: microscopic structuring by industrial lithography

S/N ratio in intrinsic Silicon

Signal of a mip in such a detector:

$$\frac{dE/dx \cdot d}{I_0} = \frac{3.87 \cdot 10^6\,\mathrm{eV/cm} \cdot 0.03\,\mathrm{cm}}{3.62\,\mathrm{eV}} \approx 3.2 \cdot 10^4\ e^- h^+ - \mathrm{pairs}$$

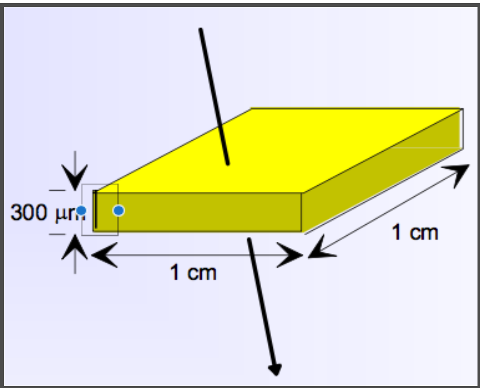

Intrinsic charge carrier (T = 300 K):

$n_i\, dA = 1.45 \cdot 10^{10}\mathrm{cm}^{-3} \cdot 0.03\mathrm{cm} \cdot 1\mathrm{cm}^2$

$\approx 4.35 \cdot 10^8$ e–h$^+$ pairs

Number of thermal created e–h+-pairs are four orders of magnitude larger than signal!!!

⇒ Need to reduce free charge carriers, i.e. deplete the detector

⇒ Most detectors make use of reverse biased p-n junctions

Silicon Detector (Reverse Bias p-n junction)

- Make the p-n junction at the surface of a silicon wafer with the bulk being n-type
- Reverse Bias to extend the depletion region throughout the n bulk

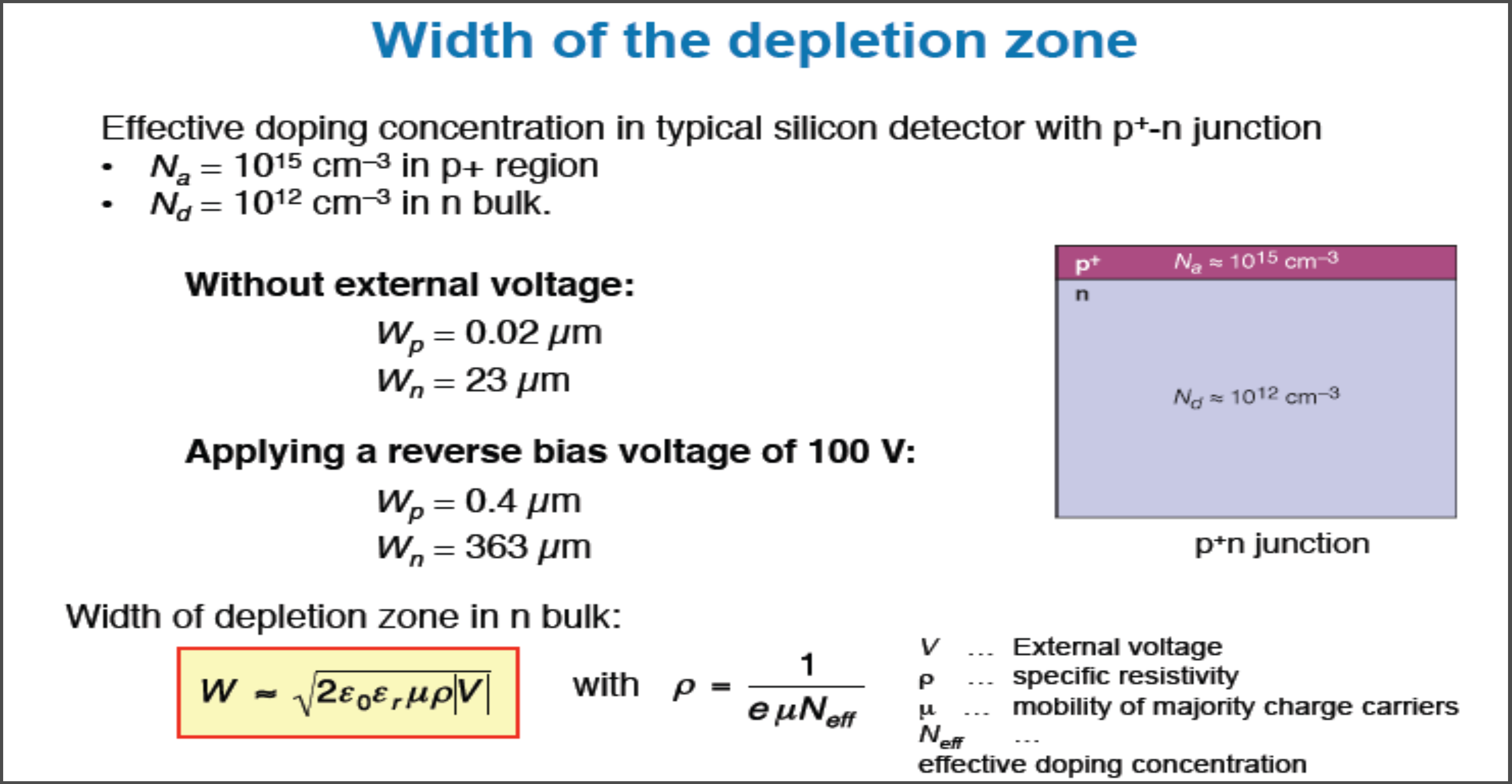

Width of the depletion zone

Effective doping concentration in typical silicon detector with p⁺-n junction

- $N_a = 10^{15}$ cm^{-3} in p+ region
- $N_d = 10^{12}$ cm^{-3} in n bulk.

Without external voltage:

$$W_p = 0.02\ \mu\text{m}$$
$$W_n = 23\ \mu\text{m}$$

Applying a reverse bias voltage of 100 V:

$$W_p = 0.4\ \mu\text{m}$$
$$W_n = 363\ \mu\text{m}$$

p⁺ $N_a \approx 10^{15}$ cm^{-3}

n

$N_d \approx 10^{12}$ cm^{-3}

p⁺n junction

Width of depletion zone in n bulk:

$$\boxed{W \approx \sqrt{2\varepsilon_0\varepsilon_r\mu\rho|V|}} \quad \text{with} \quad \rho = \frac{1}{e\,\mu N_{eff}}$$

V … External voltage
ρ … specific resistivity
μ … mobility of majority charge carriers
N_{eff} … effective doping concentration

Silicon Sensors (2)

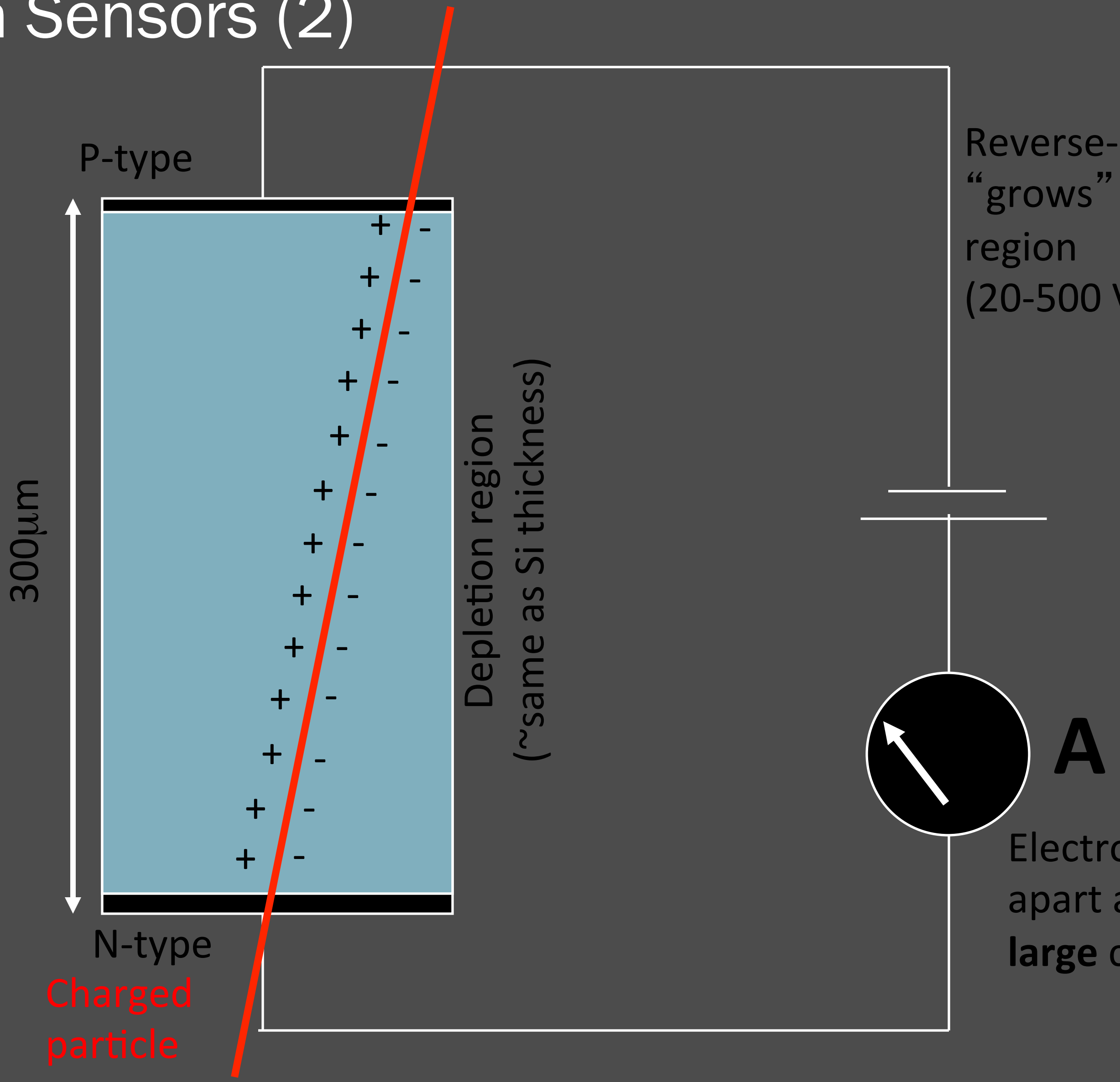

Reverse-biasing the diode "grows" the depletion region
(20-500 V required)

Electrons & holes drift apart and produce a **large** current

Principle cont..

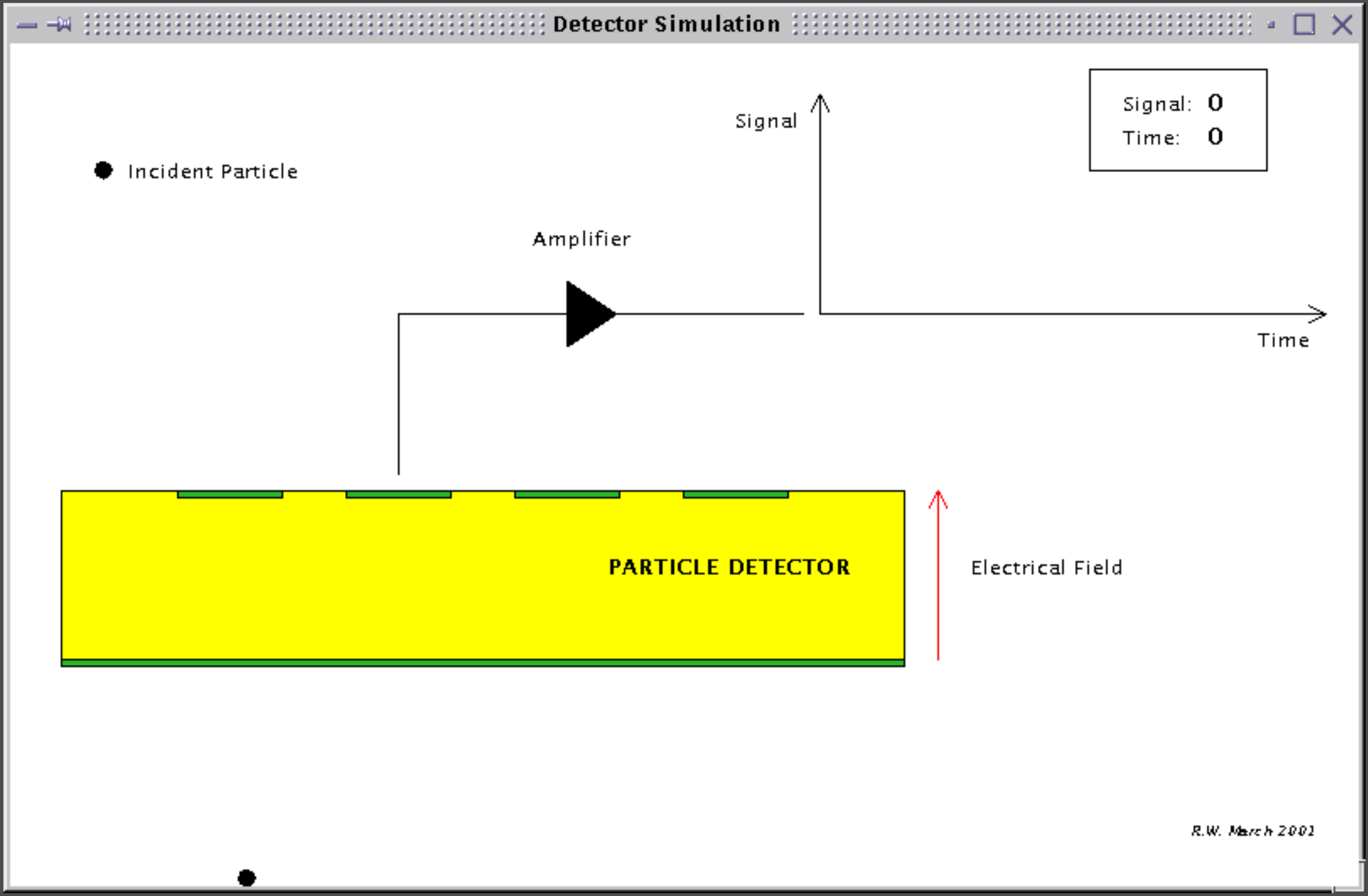

Resolution σ depends on the pitch p (distance from strip to strip)

- e.g. detection of charge in binary way (threshold discrimination) & using center of strip as measured coordinate results in $\sigma = \frac{p}{\sqrt{12}}$
- typical pitch values are 20 μm– 150 μm ⇒ 50 μm pitch results in 14.4 μm resolution

Signal to Noise Ratio

- **Landau distribution has a low energy tail**
  - becomes even lower by noise broadening

Noise sources: (ENC = Equivalent Noise Charge)

- **Capacitance** $ENC \propto C_d$
- **Leakage Current** $ENC \propto \sqrt{I}$
- **Thermal Noise** (bias resistor) $ENC \propto \sqrt{k_B T / R}$

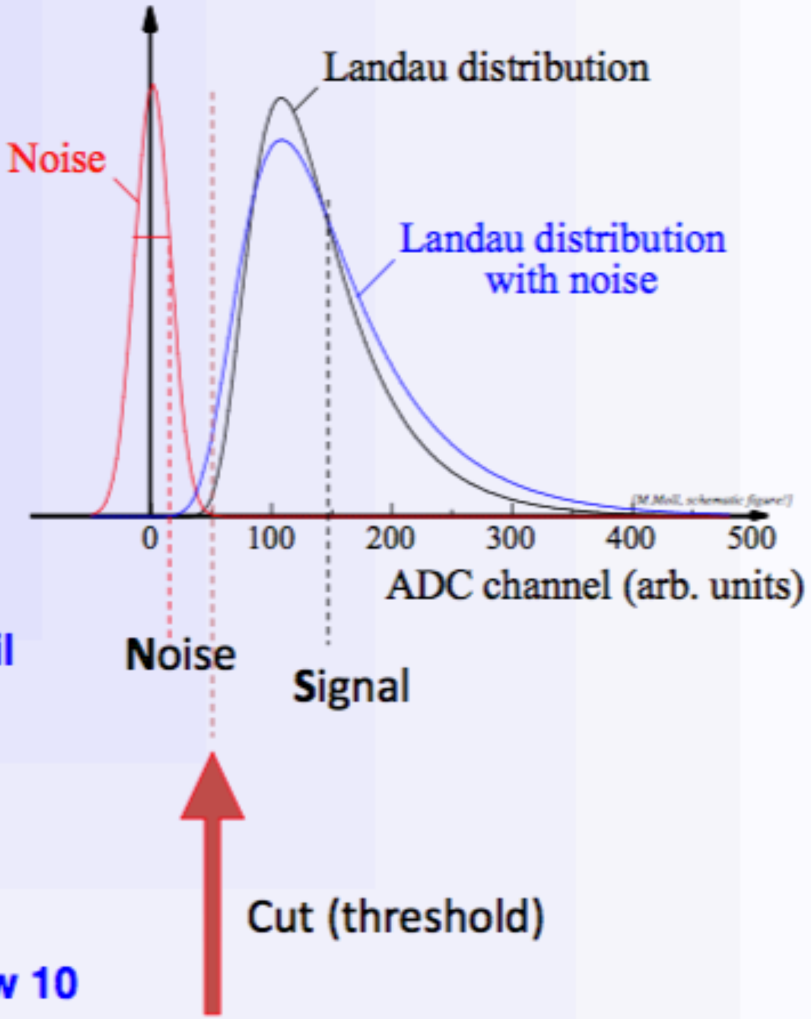

- **Good hits selected by requiring N_{ADC} > noise tail**
  - If cut too high ⇒ efficiency loss
  - If cut too low ⇒ noise occupancy

- **Figure of Merit: Signal-to-Noise Ratio S/N**

- **Typical values >10-15, people get nervous below 10**

Radiation damage severely degrades the S/N !

I-V & C-V Characterisitics

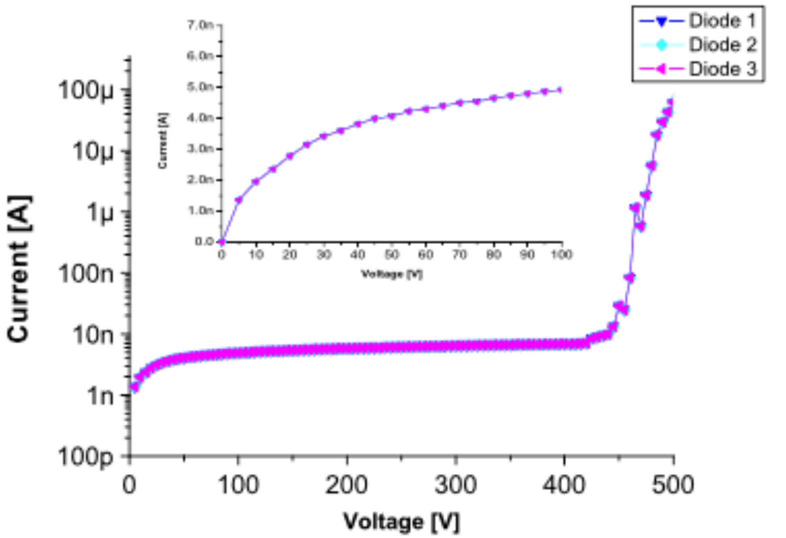

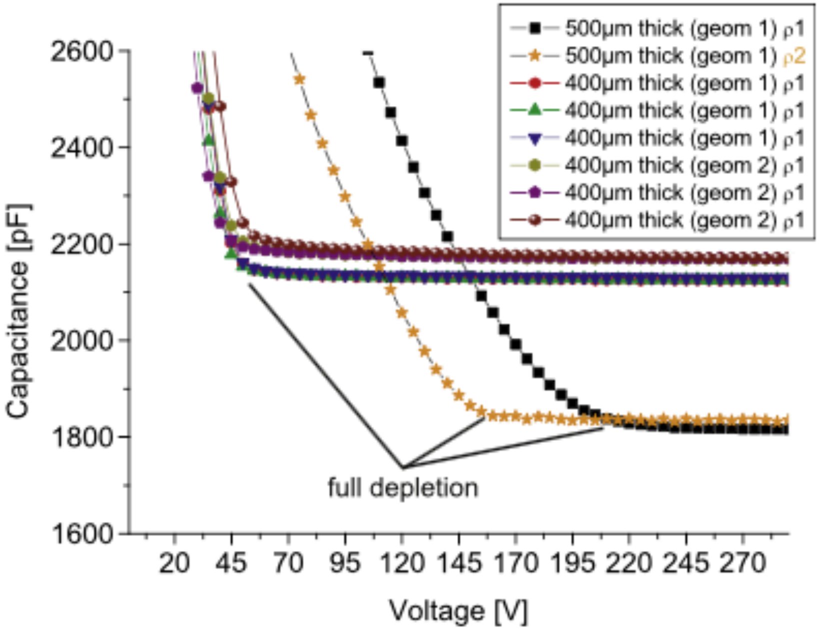

$$j_{gen} = \frac{1}{2} q \frac{n_i}{\tau_0} W \qquad j_{gen} \propto T^{3/2} \exp\left(\frac{1}{2kT}\right)$$

$$\boxed{j_{gen} \times 2 \ \ for\ \Delta T = 7K}$$

$$C_{bulk} = \begin{cases} A\sqrt{\dfrac{\epsilon_{Si}}{2\varrho\mu V_{bias}}}, & V_{bias} \leq V_{FD} \\ A\dfrac{\epsilon_{Si}}{D_{depletion}} = const., & V_{bias} > V_{FD}. \end{cases}$$

Silicon Detector Fabrication

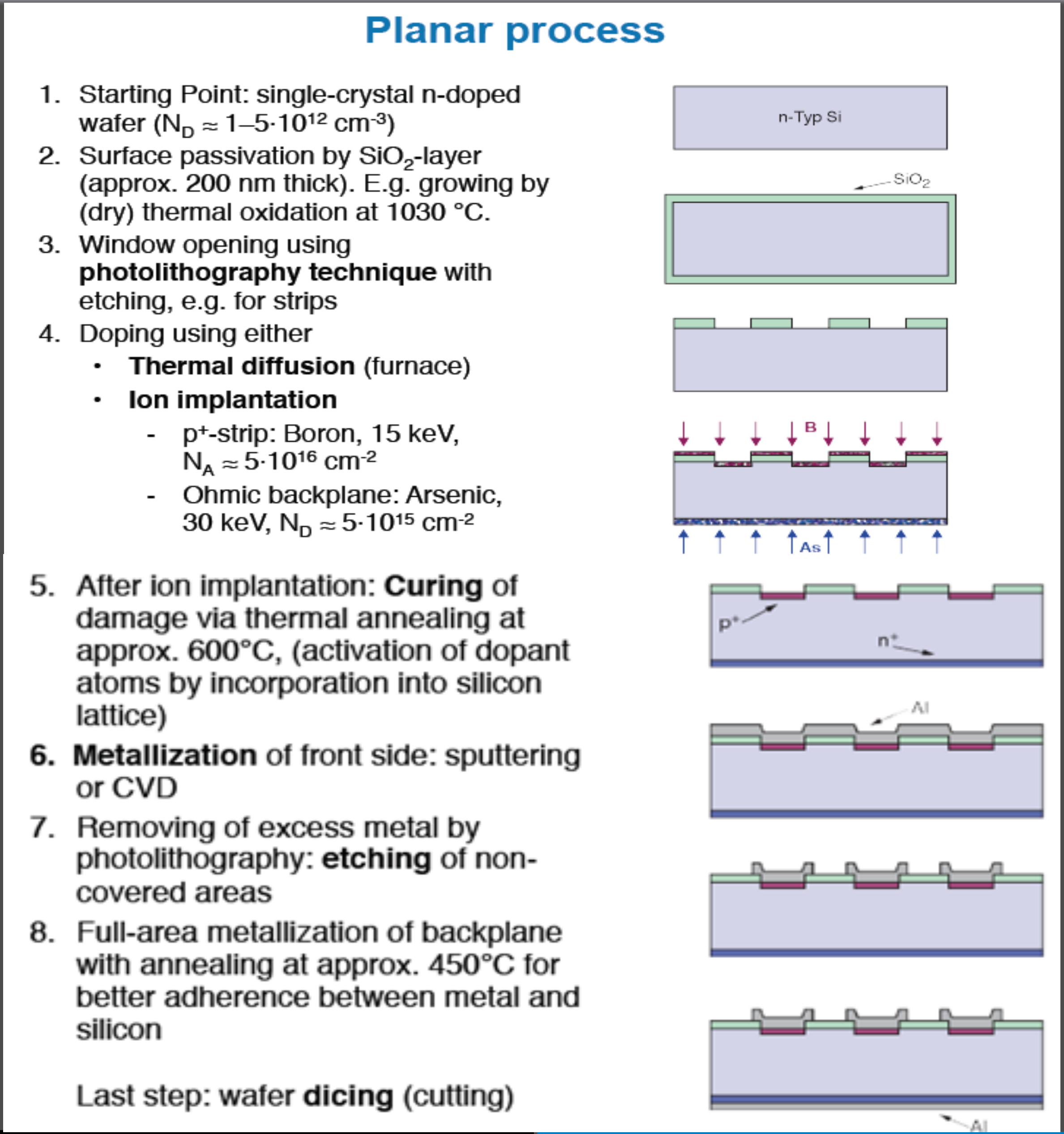

Planar process

1. Starting Point: single-crystal n-doped wafer ($N_D \approx 1\text{–}5 \cdot 10^{12}\ \mathrm{cm}^{-3}$)
2. Surface passivation by SiO$_2$-layer (approx. 200 nm thick). E.g. growing by (dry) thermal oxidation at 1030 °C.
3. Window opening using **photolithography technique** with etching, e.g. for strips
4. Doping using either
   - **Thermal diffusion** (furnace)
   - **Ion implantation**
     - p$^+$-strip: Boron, 15 keV, $N_A \approx 5 \cdot 10^{16}\ \mathrm{cm}^{-2}$
     - Ohmic backplane: Arsenic, 30 keV, $N_D \approx 5 \cdot 10^{15}\ \mathrm{cm}^{-2}$
5. After ion implantation: **Curing** of damage via thermal annealing at approx. 600°C, (activation of dopant atoms by incorporation into silicon lattice)
6. **Metallization** of front side: sputtering or CVD
7. Removing of excess metal by photolithography: **etching** of non-covered areas
8. Full-area metallization of backplane with annealing at approx. 450°C for better adherence between metal and silicon

Last step: wafer **dicing** (cutting)

CMS Preshower Detector (DU Contribution)

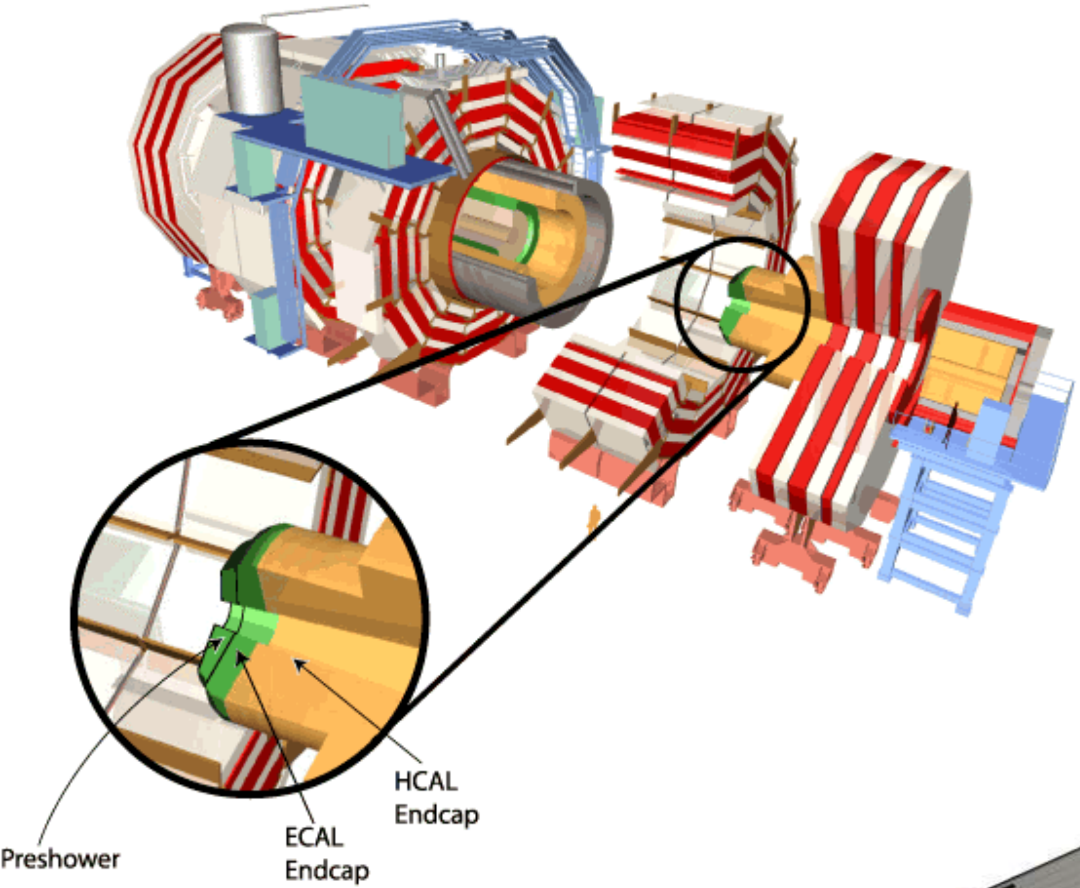

- No constraints on the support material
- Si sensors and front-end hybrids glued to a ceramics support
- Everything supported by an Al tile
- Cooling through the tile
- Si sensor: 63×63 mm^2
- 32 strips, 1.9 mm pitch
- 4300 modules, 18 m^2 of silicon

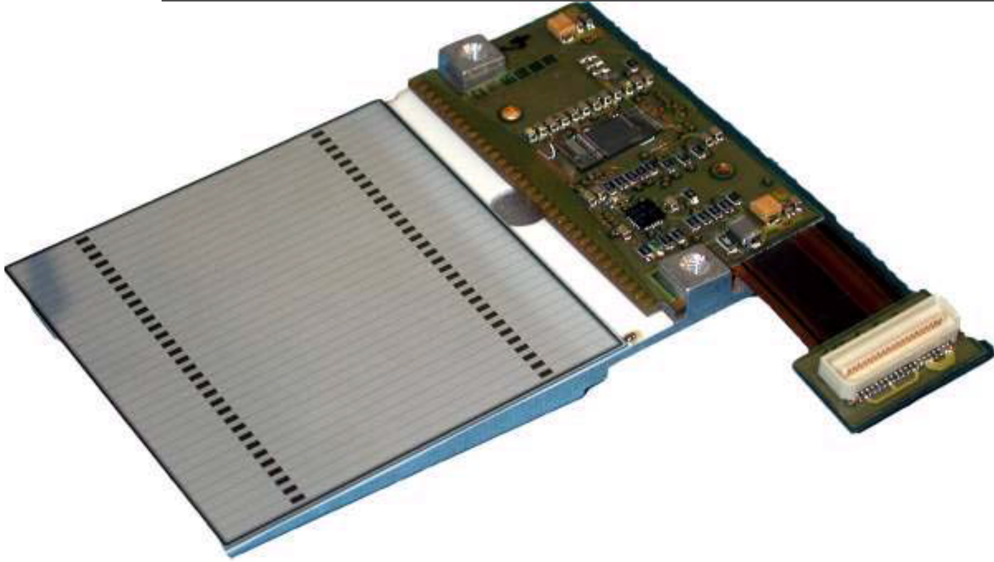

Different Configurations

Pad Detector

The most simple detector is a large surface diode with guard ring(s).

- no position resolution
- Good for basic tests (IV, CV)

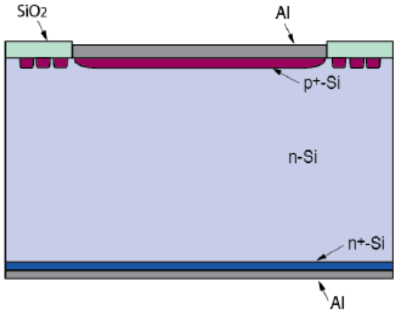

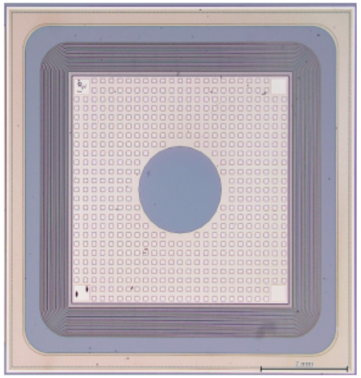

Pixel Detectors Advantages

- Double sided strip sensors produce ghost hits
  - Problematic for high occupancies
- Pixel detectors produce unambiguous hits

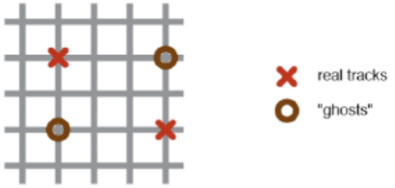

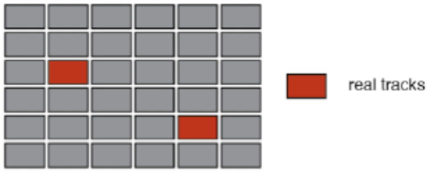

- Small pixel area → low detector capacitance (≈1 fF/Pixel) → large signal-to-noise ratio (e.g. 150:1).
- Small pixel volume → low leakage current (≈1 pA/Pixel)

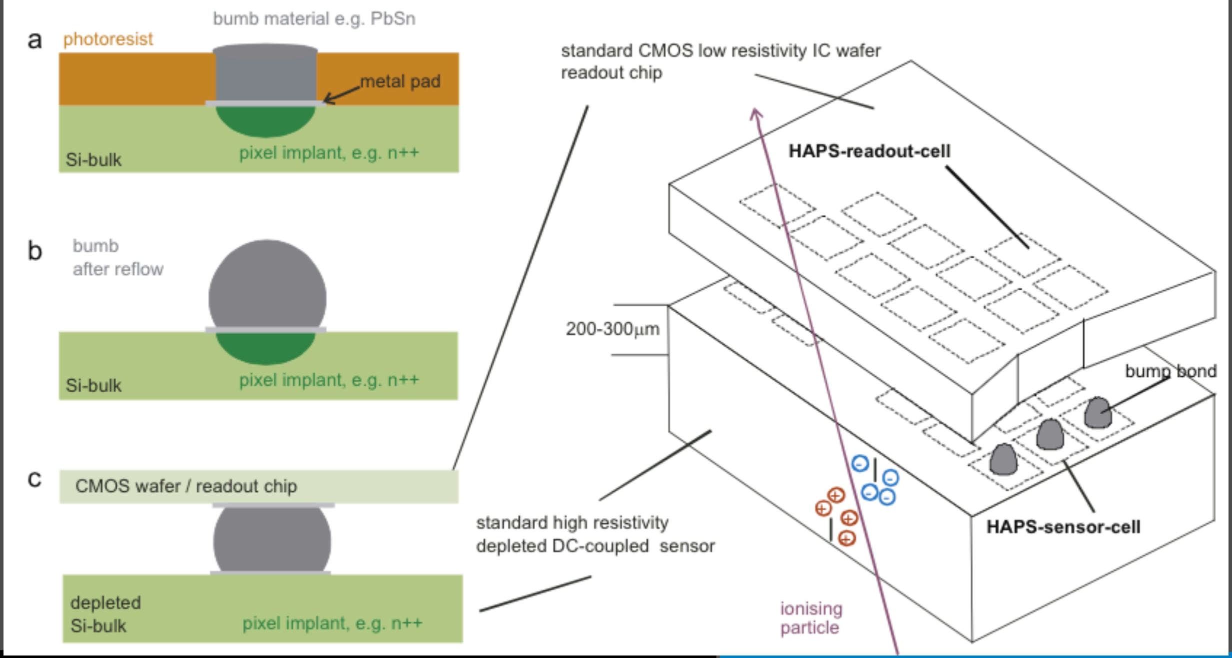

Strip Detectors

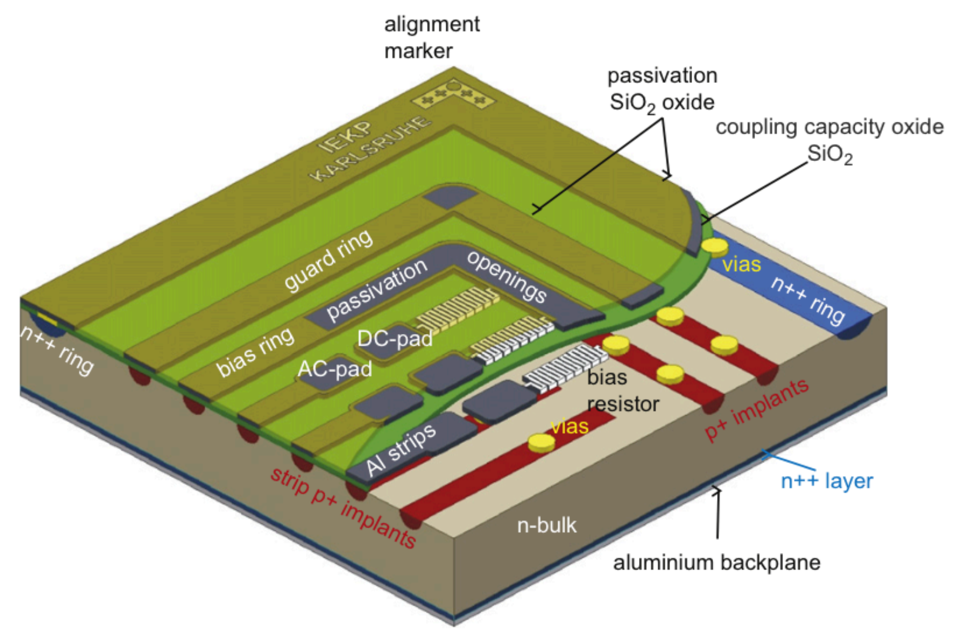

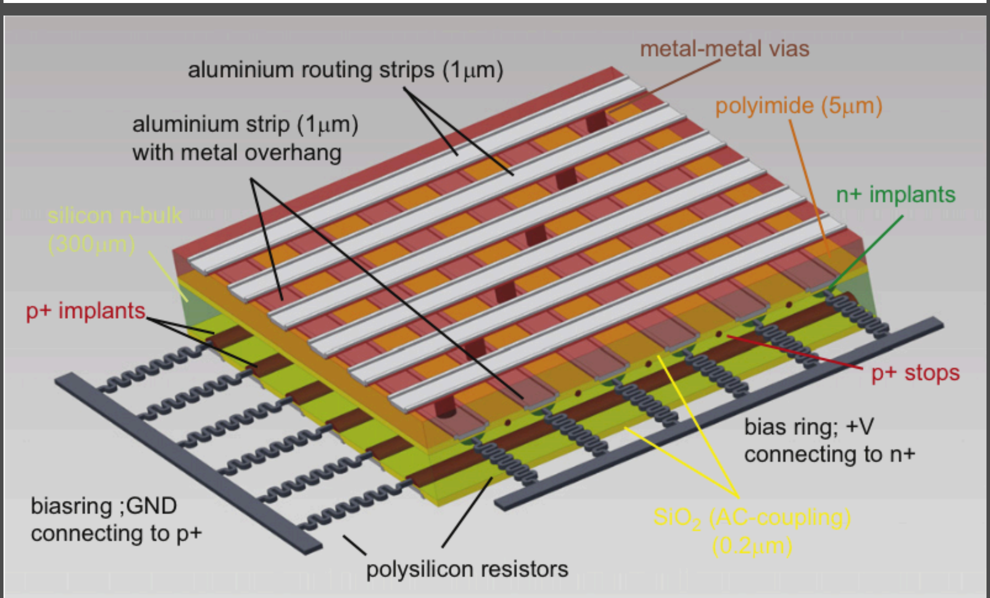

Single sided Strip Detectors

For tracking. Provides 1-D information.

Double sided Strip Detectors

For tracking. Provides 2-D information.

Radiation Damage

Surface damage (Ionizing Energy Loss):

- Build up of oxide charges, border and interface traps
  - ➡ Increase of surface current
  - ➡ Change of electrical field near to the Si-SiO_2 interface
  - ➡ Trapping near to the Si-SiO_2 interface
- C-V/I-V on MOS capacitors, MOSFET and gate controlled diodes

Bulk damage (NIEL):

- Point and cluster defects in the silicon lattice
  - ➡ Increase of leakage current
  - ➡ Change of the space charge in the depletion region, increase of full depletion voltage
  - ➡ Trapping of drifting charge
- I-V, C-V and CCE on pad diodes

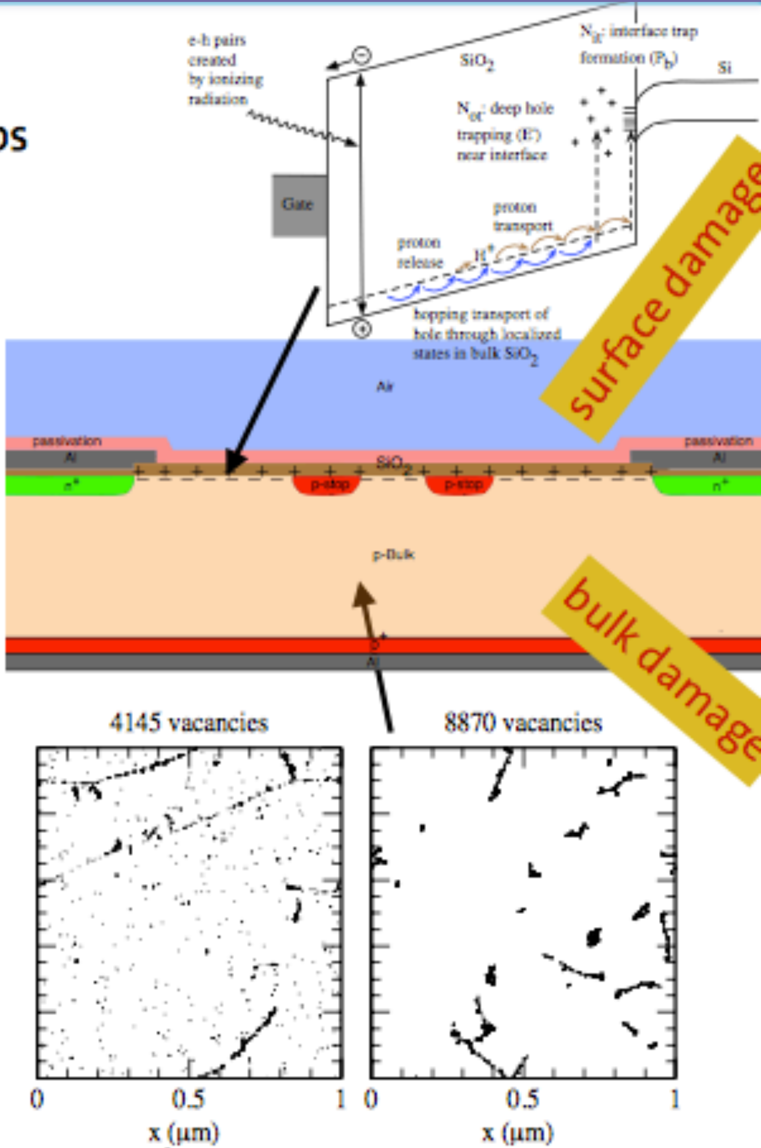

24 GeV/c protons 1 MeV neutrons

Radiation Damage: BulkDamage

- Damage models
  - ☐ fill the simulators with identified levels (convergance problems in simulators)
  - ☐ use effective trap levels (2 or 3, not many more)

  to model the large number of traps levels

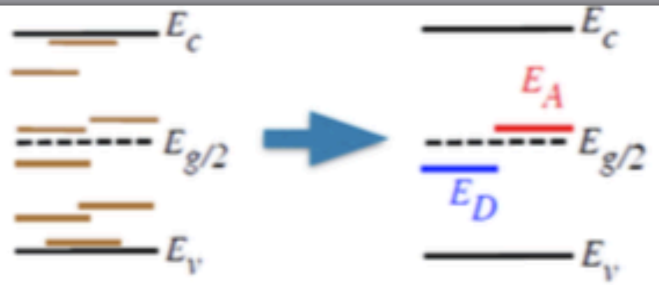

- Assume the traps obey SRH statistics:

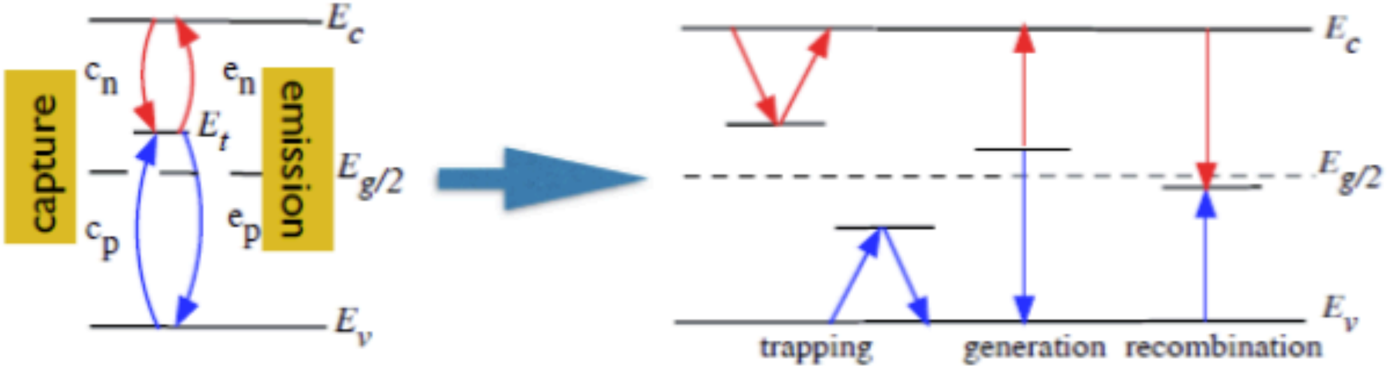

- Any trap level included in simulation requires 4 parameters:
  - ☐ defect concentration – function of fluence
  - ☐ cross sections for hole and electron capture
  - ☐ energy level

Parameters should be precisely known or amount of traps should be small.

Macroscopic Effects of Bulk Damage

…. with particle fluence:

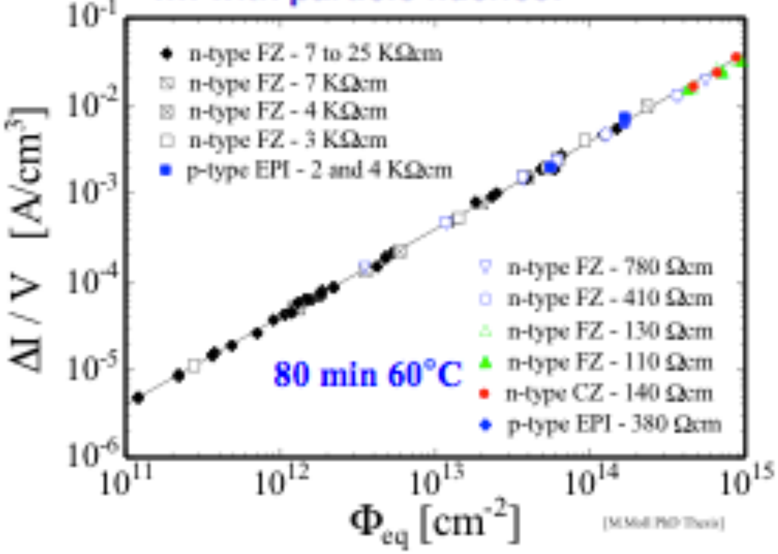

- Damage parameter α (slope in figure)

$$\boxed{\alpha = \frac{\Delta I}{V \cdot \Phi_{eq}}}$$

Leakage current per unit volume and particle fluence

- α is constant over several orders of fluence and independent of impurity concentration in Si
  ⇨ can be used for fluence measurement

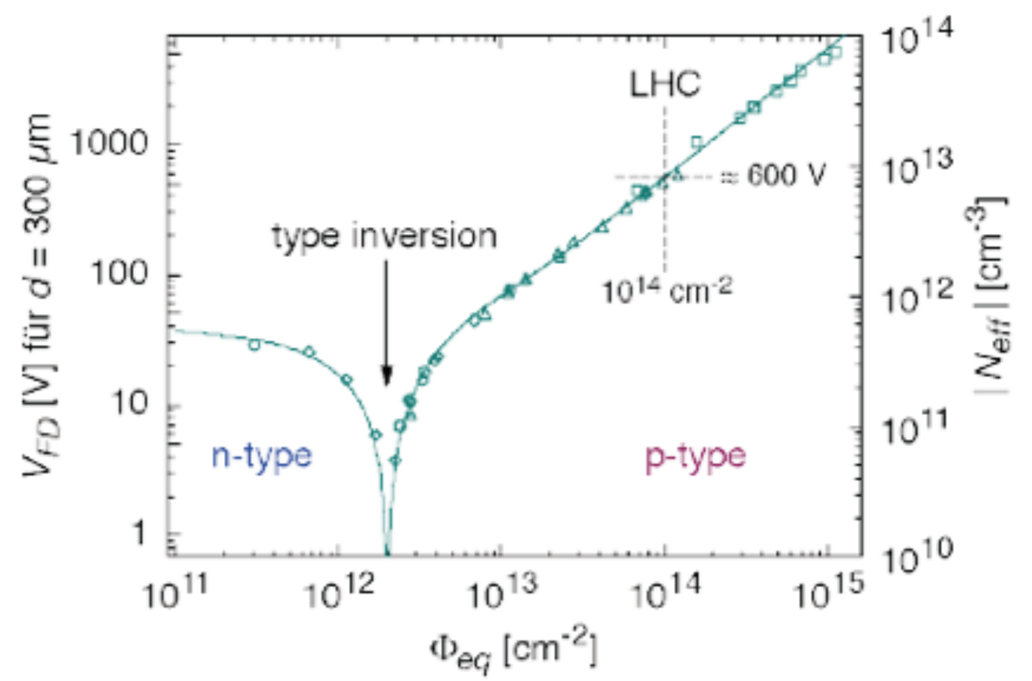

HL-LHC Environment

LHC to undergo upgrade in year 2022 → High Luminosity - LHC

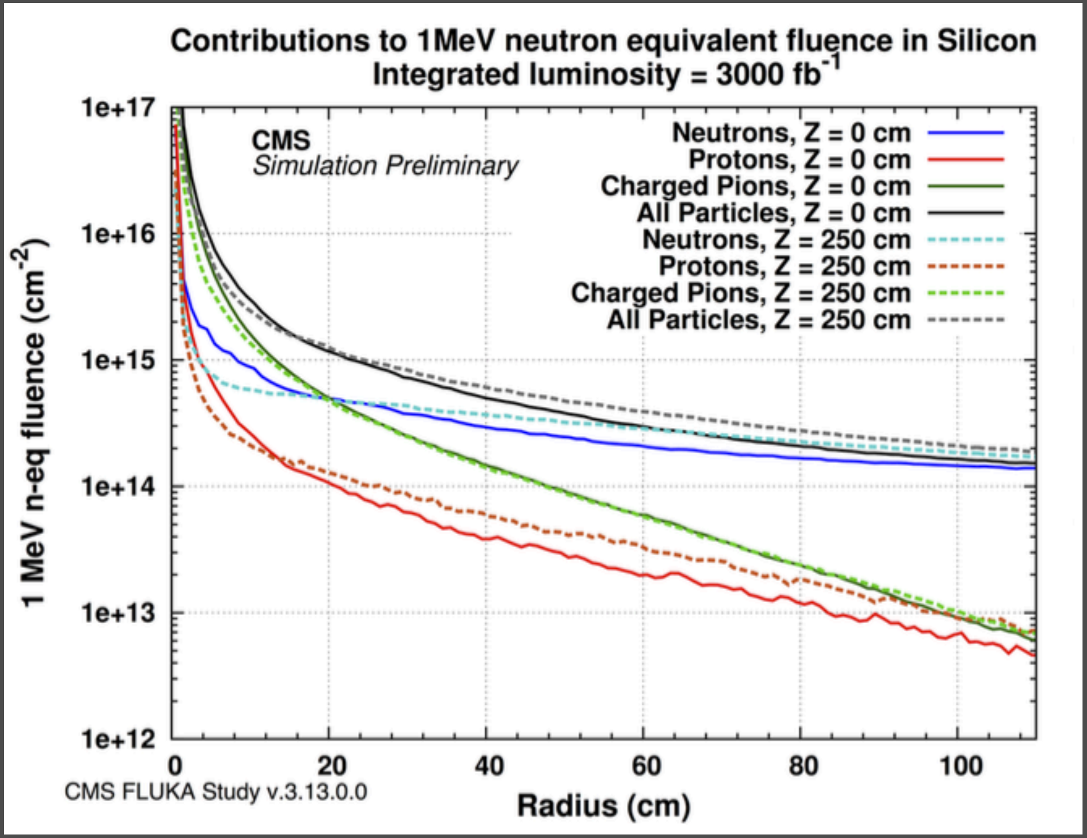

The current tracker can not survive in HL-LHC ! ☹

↓

A 'NEW TRACKER' is required !!

New Tracker: Radiation hard material, granular → Material growth techniques, substrate, implant, configuration, thickness, geometry are crucial parameters

* H. Behnanian. 13th IPRD. 2014 JINST 9 C04033

HPK Campaign

Optimization in multi-parameter space (164 wafers):

→Si bulk material, thickness, polarity, layout-parameters like strip pitch, etc.

→ Have one company implement identical structures on different silicon wafers:

→ n-type and p-type(with p-stop and p-spray strip isolation)

→ Characterizations are done before and after irradiations (both with 23MeV protons @ KIT and reactor neutrons @ JSI, Ljubljana)

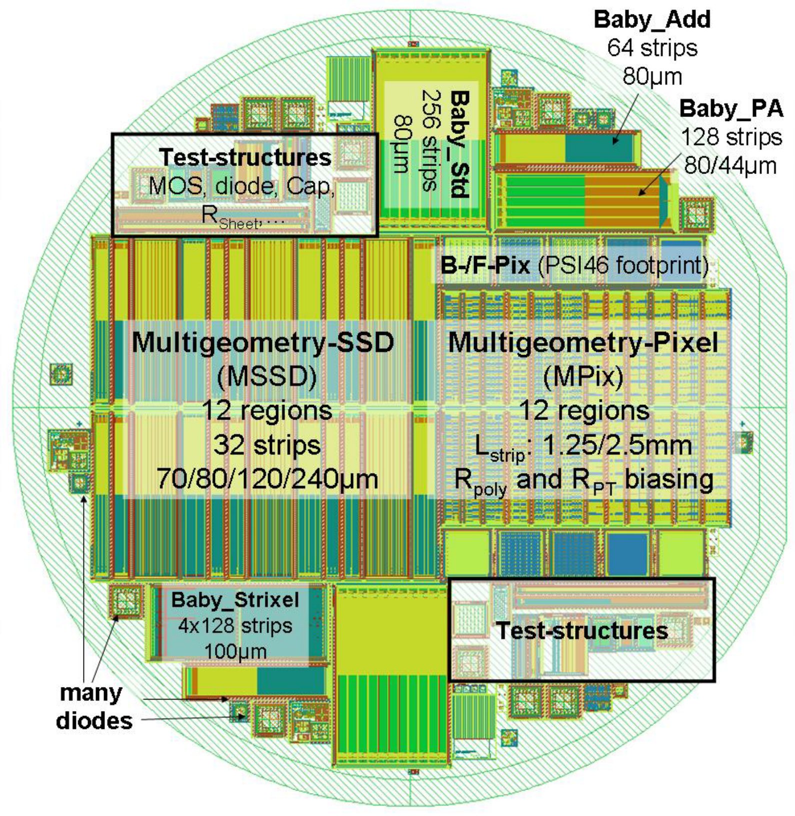

DU’s Contribution in Outer Tracker

- CMS Phase II Tracker R&D for Si strip sensors is done under HPK Campaign
- MSSD measurement results are complemented with TCAD device simulation
  - Excellent agreement of C_{int} with un-irradiated sensors
  - Comparison with both n-type and p-type substrates
  - R&D for p-stop/p-spray design is ongoing
- Trap model developed and further R&D for Radiation Damage simulation is in progress
  - effects on leakage current, full depletion voltage, Charge collection efficiency and double peak electric field effect are in agreement
- 2-D simulation for pixel sensors is performed

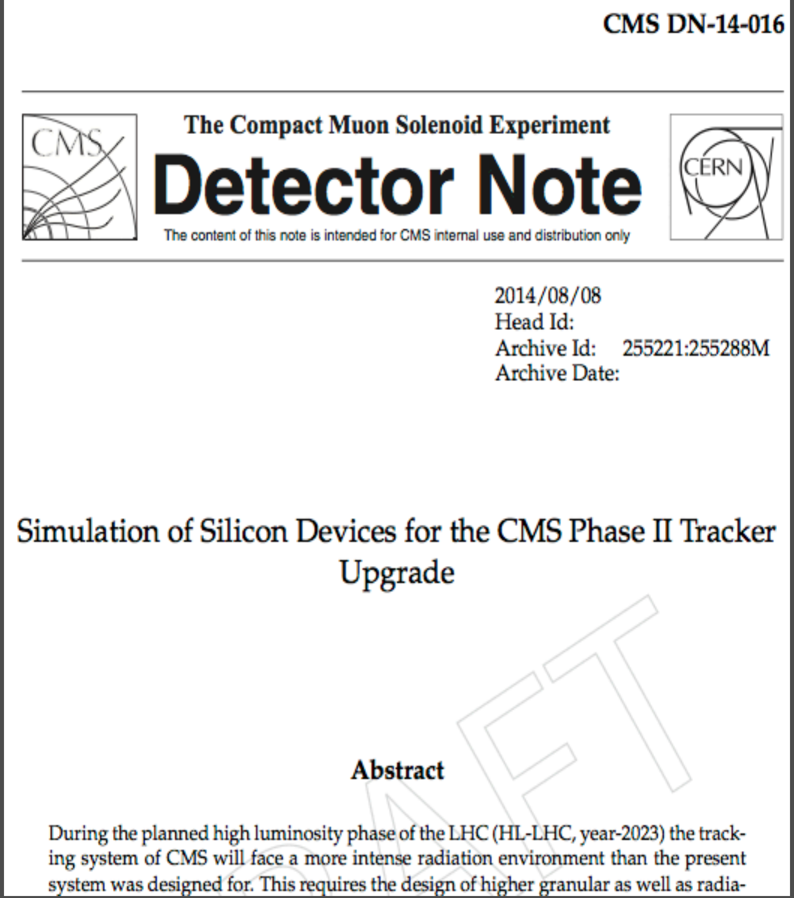

CMS DN-14-016

The Compact Muon Solenoid Experiment

Detector Note

The content of this note is intended for CMS internal use and distribution only

2014/08/08
Head Id:
Archive Id: 255221:255288M
Archive Date:

Simulation of Silicon Devices for the CMS Phase II Tracker Upgrade

Abstract

During the planned high luminosity phase of the LHC (HL-LHC, year-2023) the tracking system of CMS will face a more intense radiation environment than the present system was designed for. This requires the design of higher granular as well as radia-

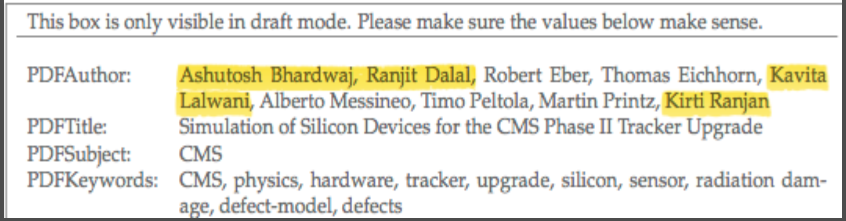

This box is only visible in draft mode. Please make sure the values below make sense.

PDFAuthor: Ashutosh Bhardwaj, Ranjit Dalal, Robert Eber, Thomas Eichhorn, Kavita Lalwani, Alberto Messineo, Timo Peltola, Martin Printz, Kirti Ranjan
PDFTitle: Simulation of Silicon Devices for the CMS Phase II Tracker Upgrade
PDFSubject: CMS
PDFKeywords: CMS, physics, hardware, tracker, upgrade, silicon, sensor, radiation damage, defect-model, defects

Charge Collection Efficiency: P-type OR N-type substrate

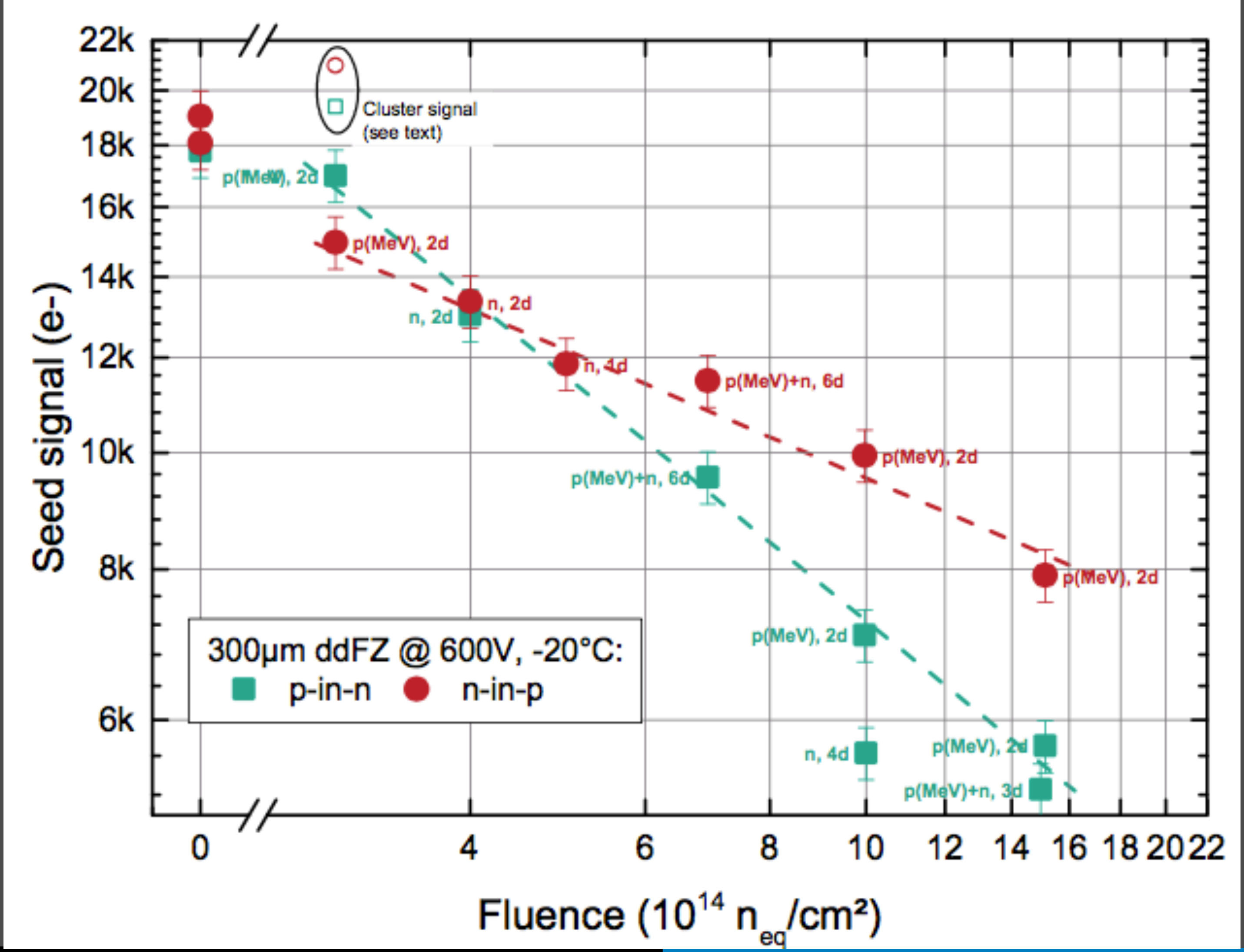

Noise Distribution: Gaussian Fitted

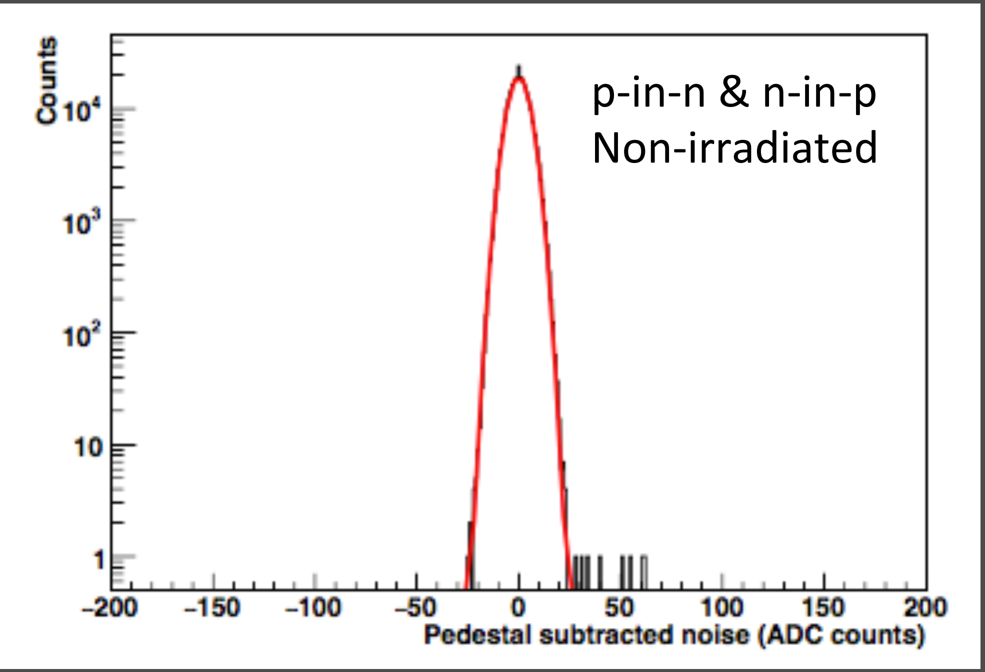

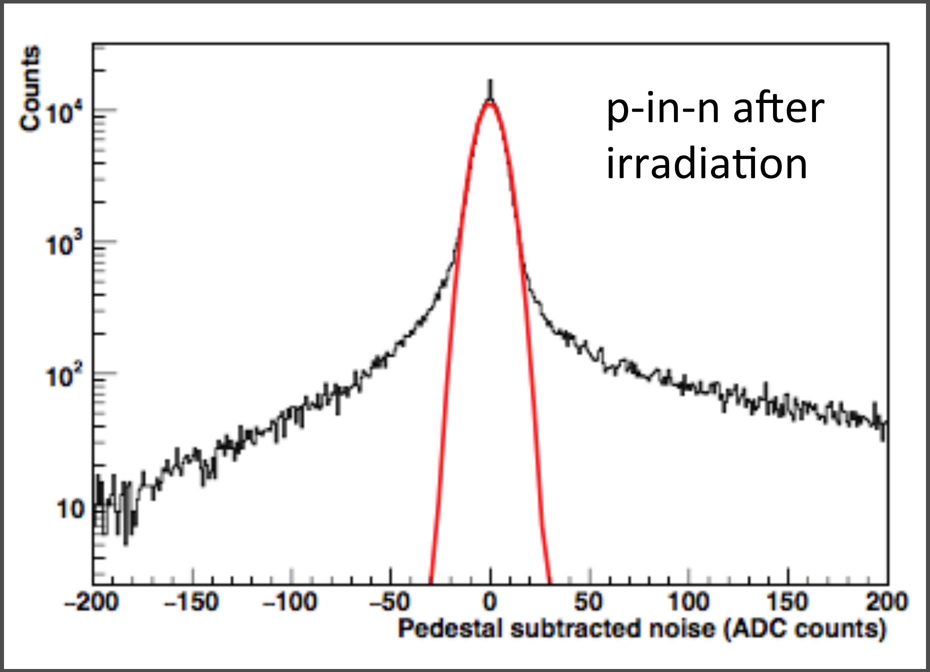

Recent models for p-bulk – New Delhi model

Ranjeet Dalal et al., PoS(Vertex2014)030

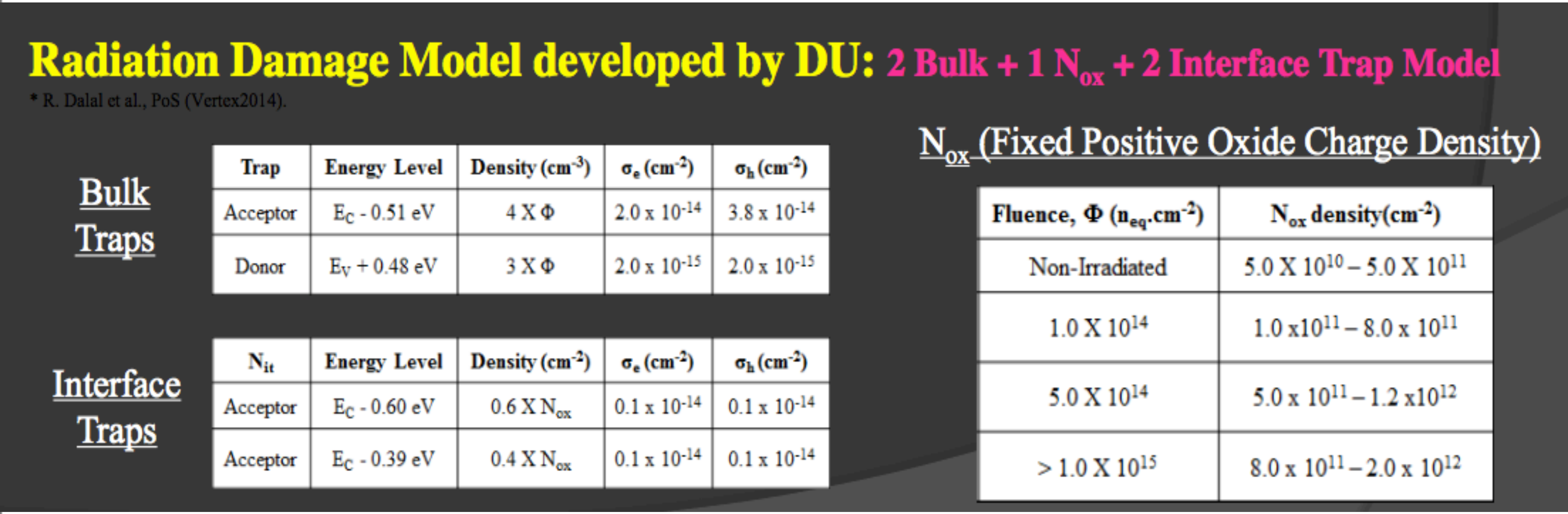

Radiation Damage Model developed by DU: 2 Bulk + 1 N_{ox} + 2 Interface Trap Model

* R. Dalal et al., PoS (Vertex2014).

Bulk Traps

Trap	Energy Level	Density (cm^{-3})	σ_e (cm^{-2})	σ_h (cm^{-2})
Acceptor	E_C - 0.51 eV	4 X Φ	2.0×10^{-14}	3.8×10^{-14}
Donor	E_V + 0.48 eV	3 X Φ	2.0×10^{-15}	2.0×10^{-15}

Interface Traps

N_{it}	Energy Level	Density (cm^{-2})	σ_e (cm^{-2})	σ_h (cm^{-2})
Acceptor	E_C - 0.60 eV	0.6 X N_{ox}	0.1×10^{-14}	0.1×10^{-14}
Acceptor	E_C - 0.39 eV	0.4 X N_{ox}	0.1×10^{-14}	0.1×10^{-14}

N_{ox} (Fixed Positive Oxide Charge Density)

Fluence, Φ ($n_{eq}.cm^{-2}$)	N_{ox} density(cm^{-2})
Non-Irradiated	$5.0 \times 10^{10} – 5.0 \times 10^{11}$
1.0×10^{14}	$1.0 \times 10^{11} – 8.0 \times 10^{11}$
5.0×10^{14}	$5.0 \times 10^{11} – 1.2 \times 10^{12}$
$> 1.0 \times 10^{15}$	$8.0 \times 10^{11} – 2.0 \times 10^{12}$

Developed on Silvaco

Model based on the original work of:
V.Eremin, E.Verbitskaya, Z.Li, NIMA 476 (2002) 556-564

Electric Field: P-type OR N-type substrate

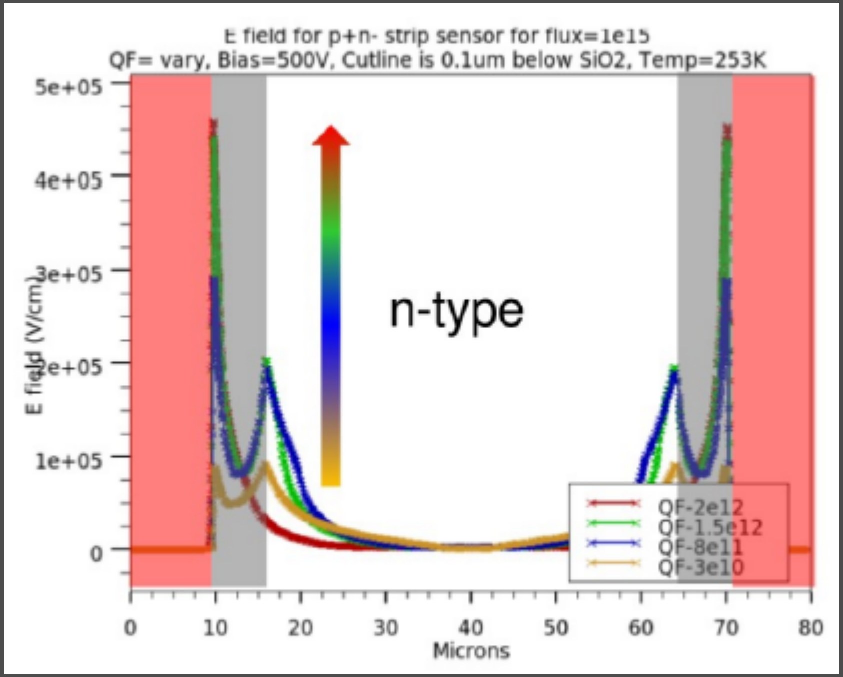

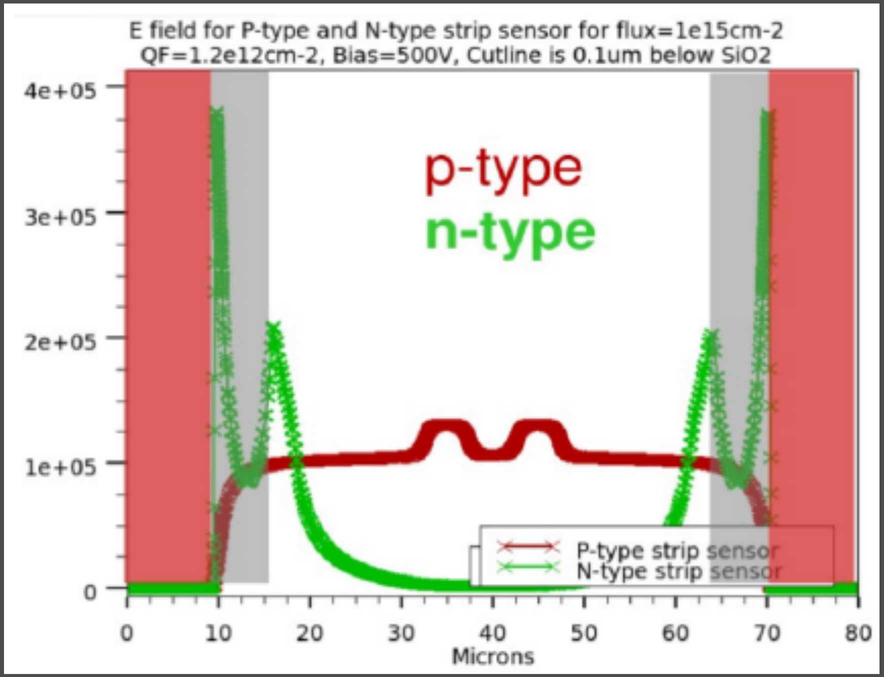

Increasing fluence → More radiation damage → Higher bulk & surface damage → Q_F grows → E.Field @ implant edges shoots!

Reverse effect of Q_F on E.Field for p-type substrates. Increase in Q_F, decreases E.Field!

* R. Ranjeet et al., Simulations for Hadron Irradiated n+p- Si Strip Sensors Incorporating Bulk and Surface Damage, presented at 23rd RD50 Workshop, CERN, Switzerland (2013).

Inter-strip Resistance

R_{int} is a surface property.
→ It was thought that it is affected by surface damage (Q_F) only.

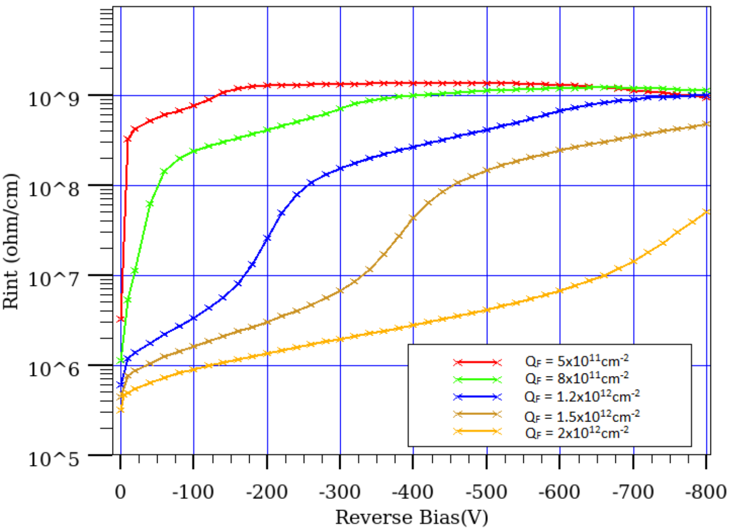

Increase in Q_F attracts more e^-s towards the n^+ side of the detector.
→ R_{int} decreases.

Not consistent with measurements!

Both surface (Q_F + N_{it}) & bulk damage traps play a role in deciding R_{int}!

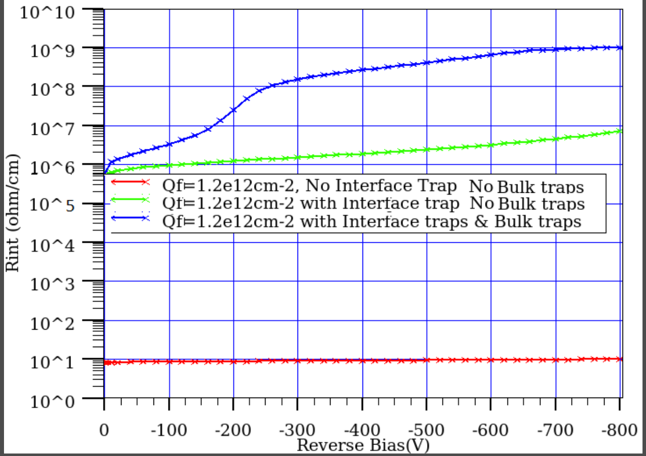

N_{it} = 2 acceptor type traps

Bulk traps = Acceptor & Donor traps, but near the n^+ implant, acceptor traps are more ionized

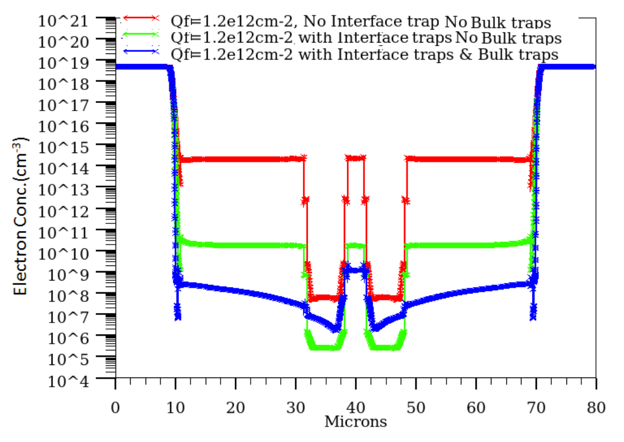

→ These two COMPENSATE the effect of accumulation of e^-s by Q_F (positive fixed oxide charge)

*R. Dalal., G. Jain, et al Simulation of Irradiated Si Detectors. POS (Vertex 2014).

India in CMS Outer Tracker- Current Status

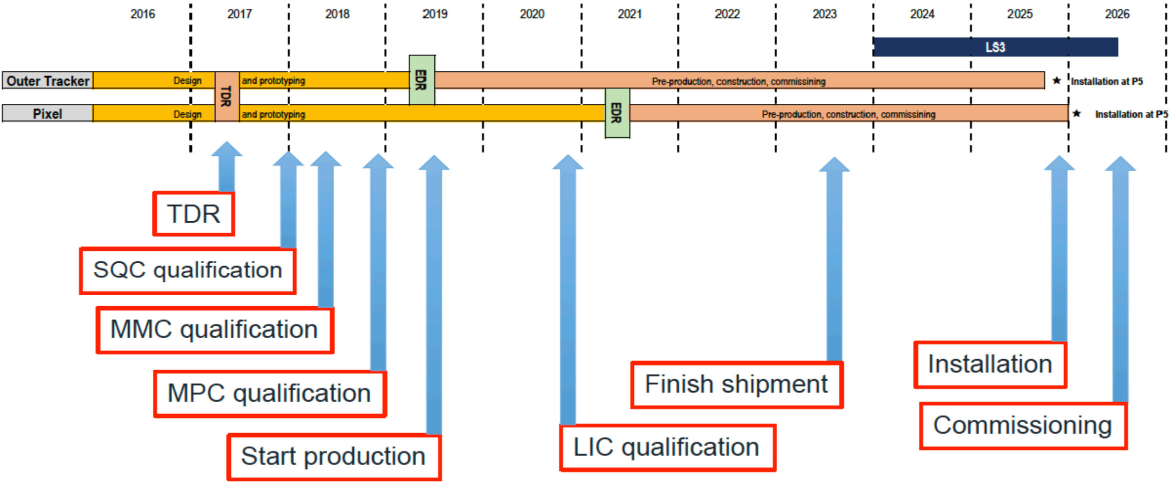

TDR

SQC qualification

MMC qualification

MPC qualification

Start production

LIC qualification

Finish shipment

Installation

Commissioning

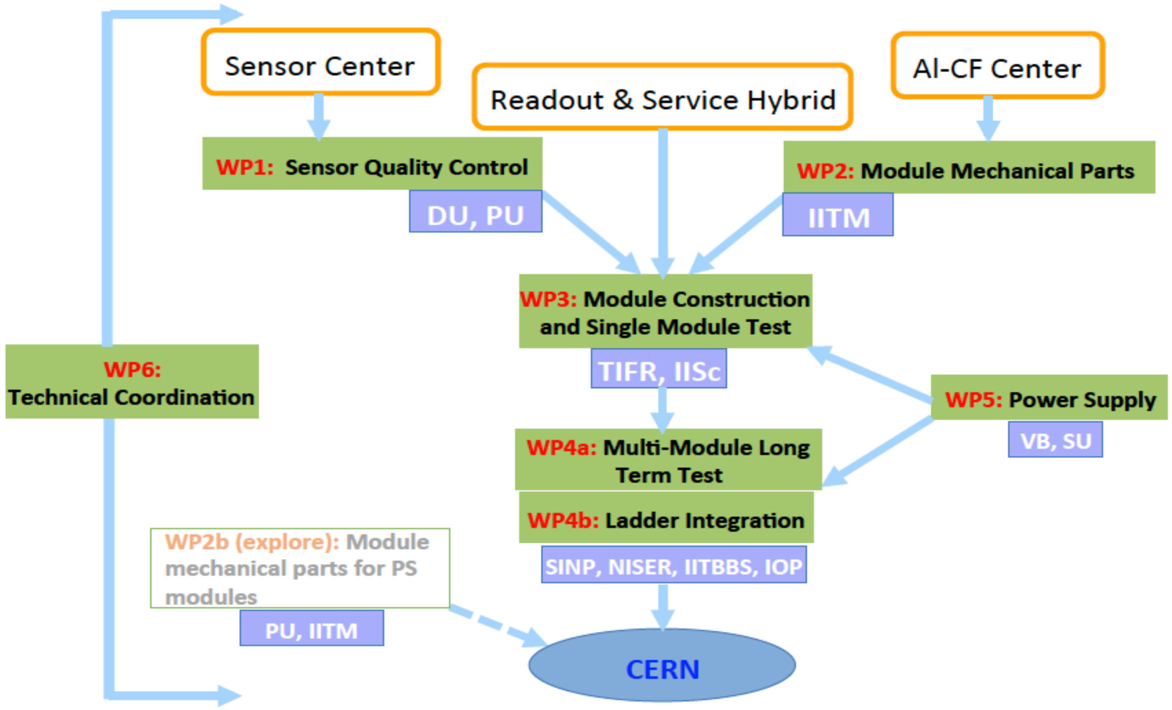

Sensor Center

Readout & Service Hybrid

Al-CF Center

WP1: Sensor Quality Control
DU, PU

WP2: Module Mechanical Parts
IITM

WP3: Module Construction and Single Module Test
TIFR, IISc

WP4a: Multi-Module Long Term Test

WP4b: Ladder Integration
SINP, NISER, IITBBS, IOP

WP5: Power Supply
VB, SU

WP6: Technical Coordination

WP2b (explore): Module mechanical parts for PS modules
PU, IITM

CERN

Acronyms used above:

SQC (Sensor Qualification Center)

MMC (Module Mechanics Center)

MPC (Module Production Center)

LIC (Ladder Integration Center)

TDR (Technical Design Report)

EDR (Engineering Design Report)

Detector Development in India

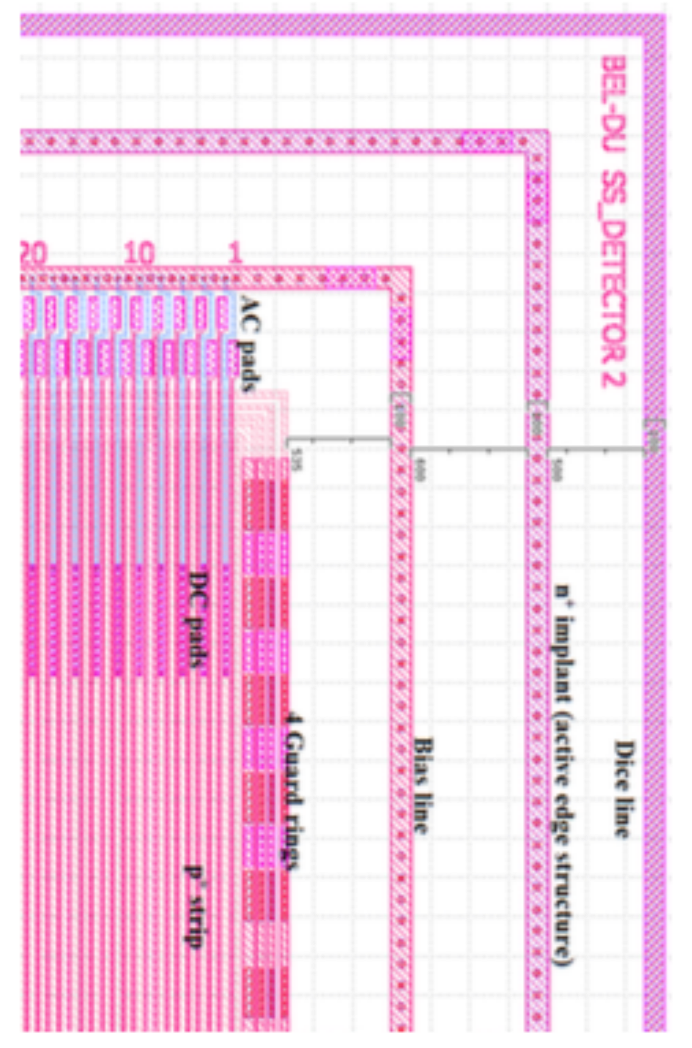

Detector Dimensions: 3.4 cm x 6.0 cm
Strip width: 30 μm, Strip pitch: 55 μm
# of Strips in each detector: 512

Measurement Results

Coupling Capacitance (specs: >110pF)

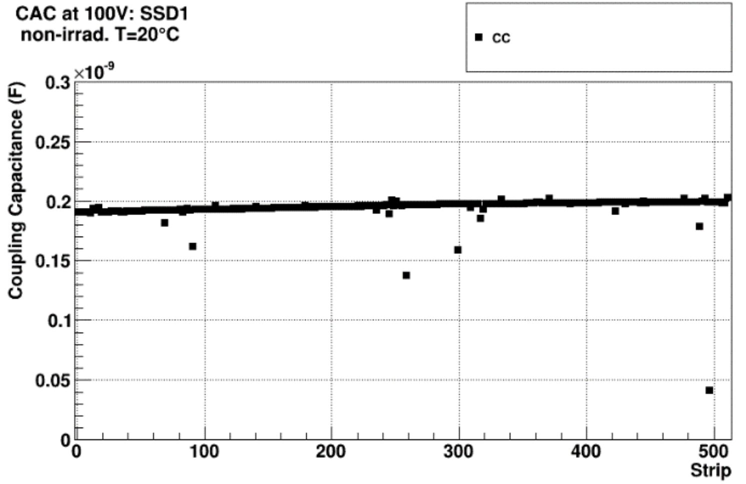

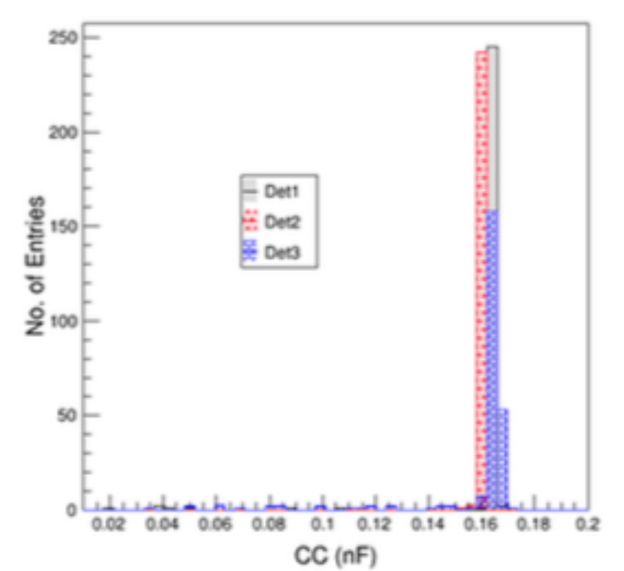

Dielectric Current (specs: < 1nA @ 10V)

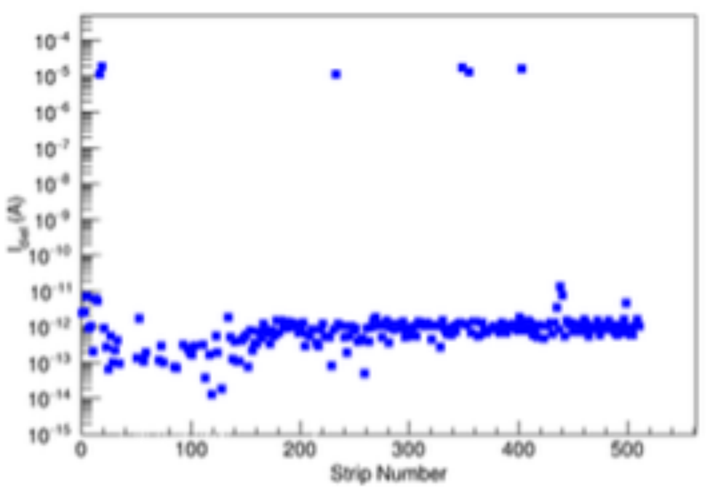

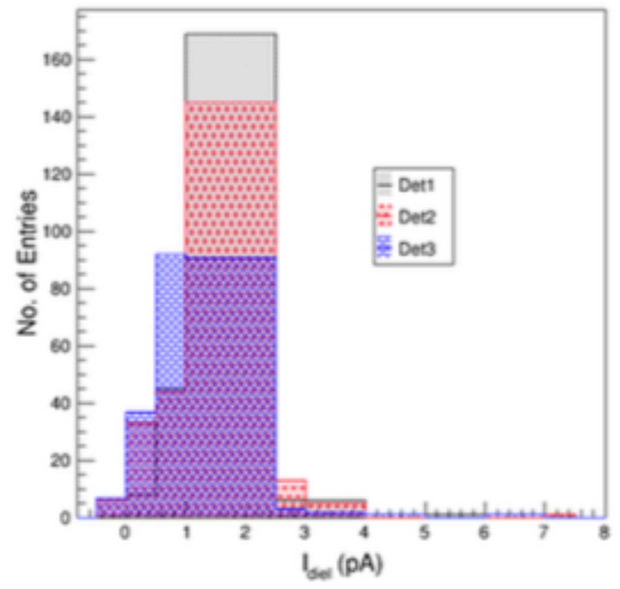

Charge Collection

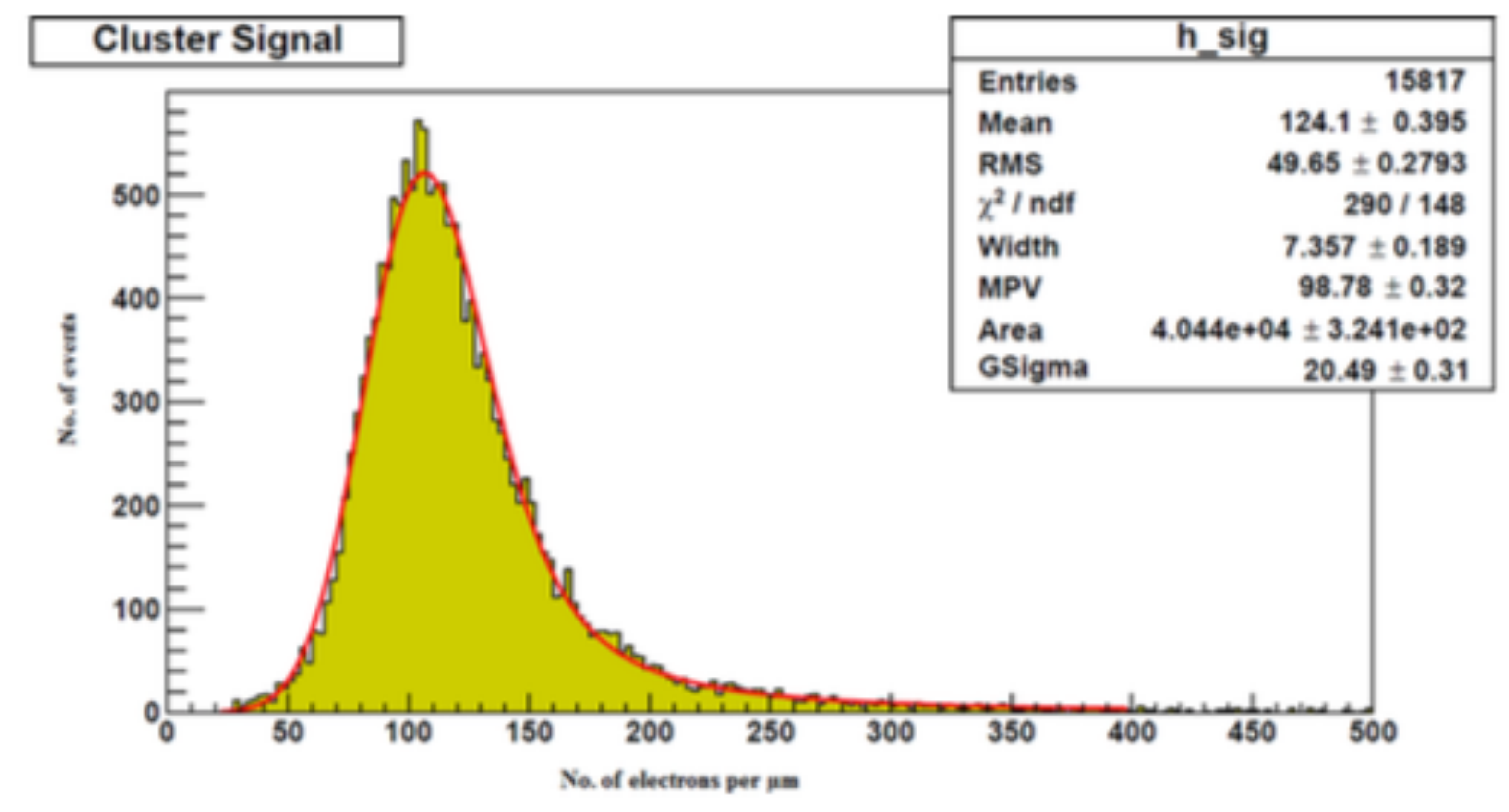

Ongoing R&D: Novel Detectors

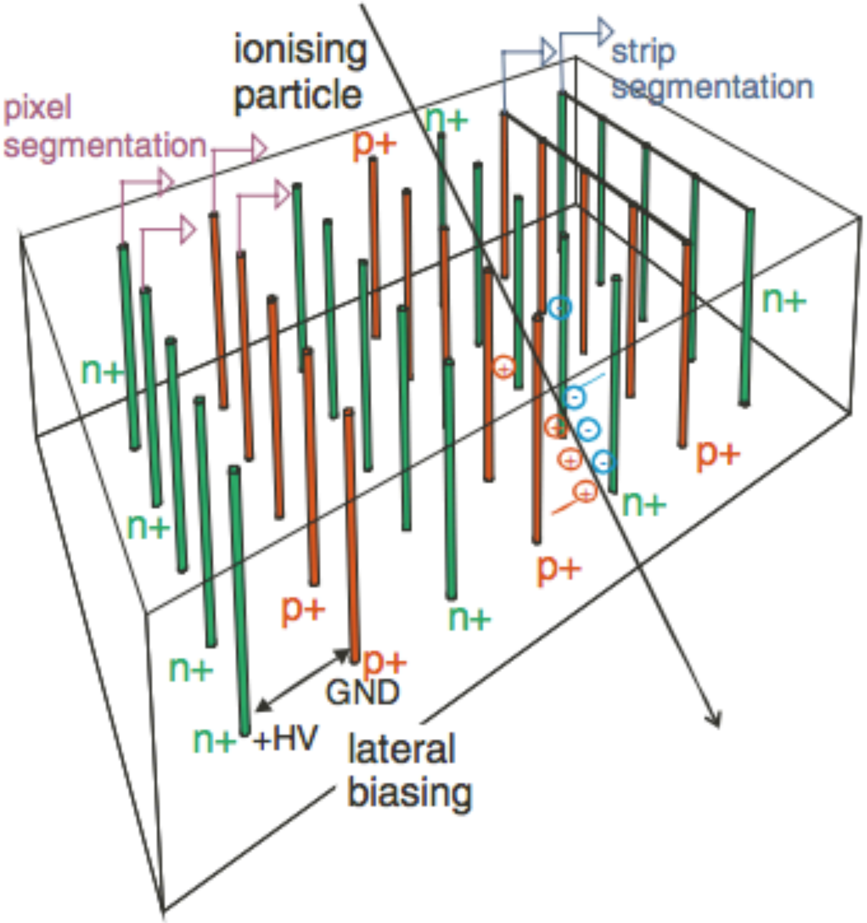

3D Columnar Detectors

Faster. Provides 2D information.

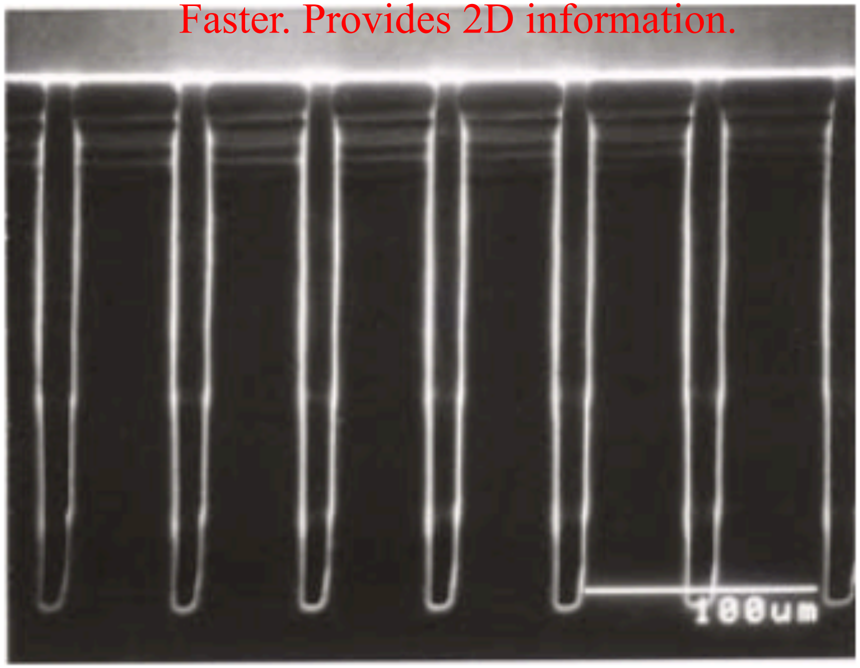

- Deep holes are etched into the silicon finally serving as electrode junctions
- The depletion zone is in the horizontal direction instead of the standard vertical one
- The electrons and holes travel a much shorter way & are therefore less sensitive to trapping.

CMOS Detectors (Monolithic Active Pixels)

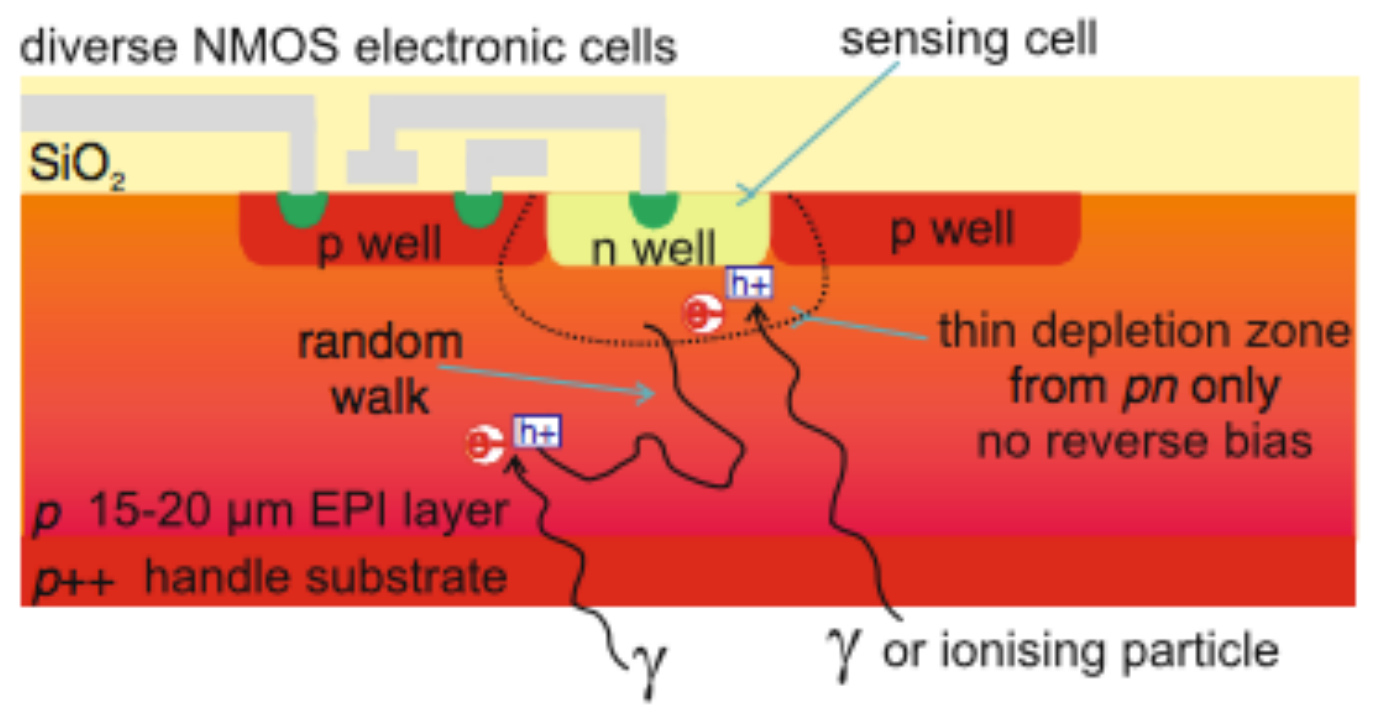

- Electrons created inside the shallow depletion zones are fully collected while electrons from the EPI layer randomly walk towards the N-well and with an excellent lifetime behaviour, only some of them will be trapped.
- Nevertheless, CMOS devices have an excellent signal-to-noise ratio due to their very small capacitances and low currents, therefore the low noise compensates for the low signal.

Low Gain Avalanche Detector

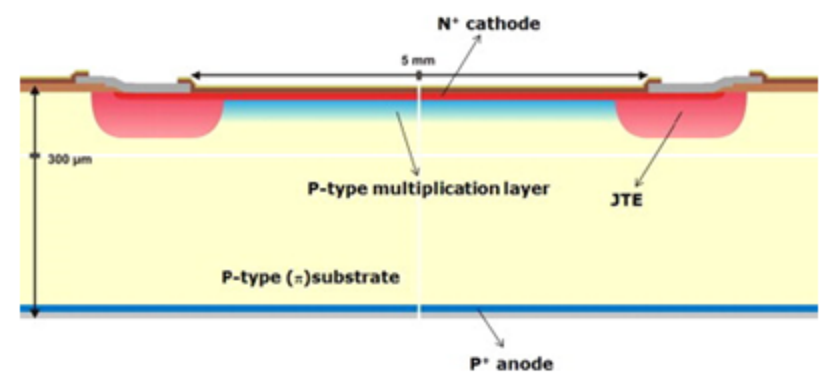

*Marta Baselga, 8th Trento workshop, 2013.

LGAD – traditional PIN detector, but with a deeper p-type multiplication layer (also called p-well) just below the n$^+$ implant.

Purpose of the p+ layer

- PN junction formed between n$^+$ implant & p-well
- A strong electric field builds in a local region
- Avalanche starts at critical electric field (> 3e5 V/cm)
- Local & controlled 'charge multiplication'
- Internal gain increases signal

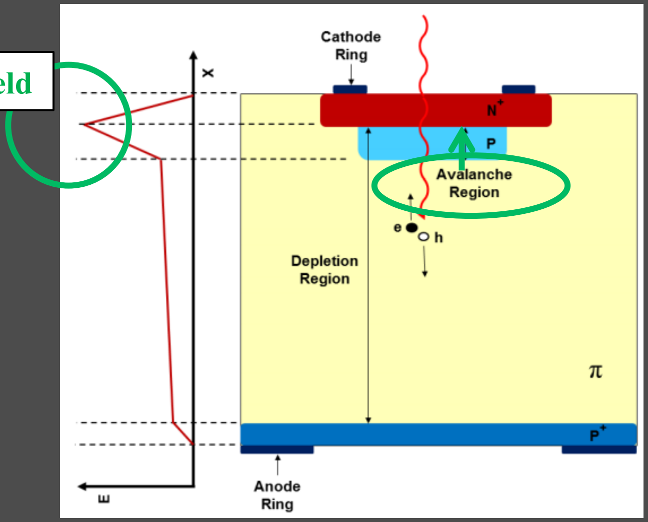

*Giulio Pellegrini, 23rd RD50 workshop.

Simulated Result: Non-Irradiated

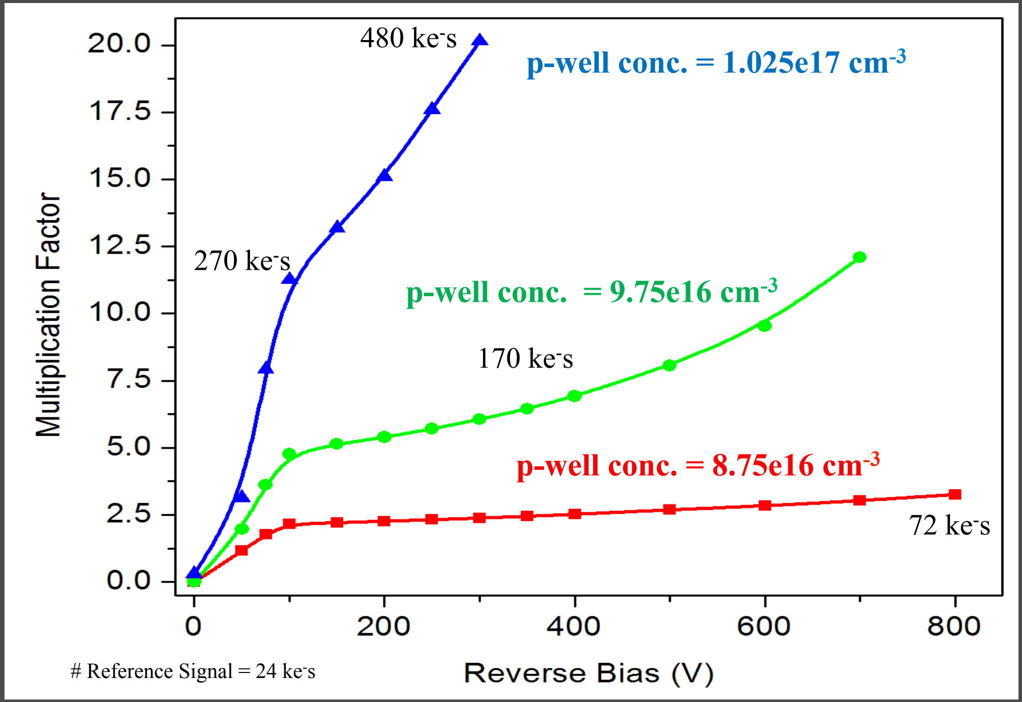

Increase in p-well conc. increases LGAD gain!

Because: increase in p-well conc. builds a stronger p-well-n^+ junction. Hence a higher peak electric field generates at the junction. This provides larger avalanche and thereby larger gain.

* R. Dalal, G. Jain, A. Bhardwaj, K. Ranjan. TCAD simulation of Low Gain Avalanche Detectors. NIM A. Manuscript accepted.

Peak E.field

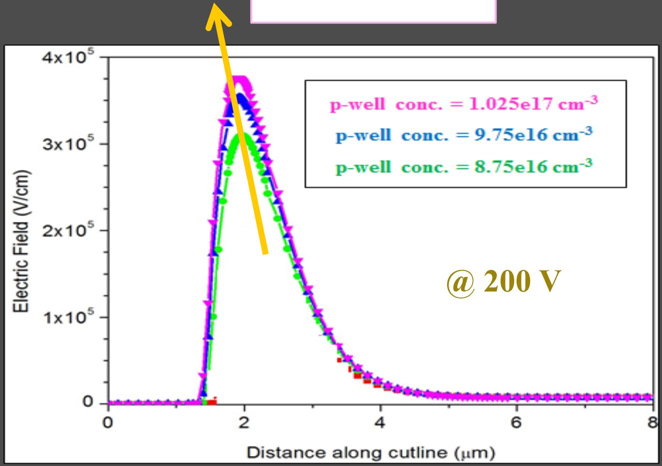

Breakdown Voltage & Gain

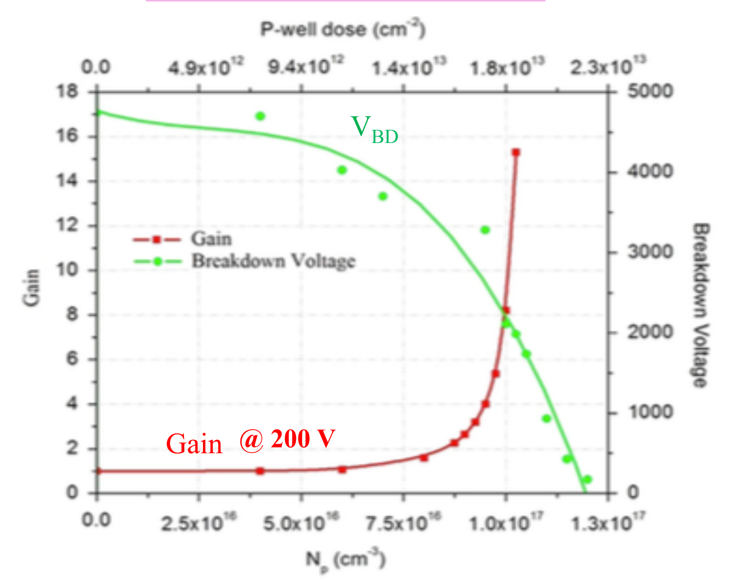

SUMMARY & Future Outlook

- Silicon sensors are widely used in HEP experiments
- Although used since more than 35 years (NA11, 1980) continuous developments enable usage in unprecedented harsh environments
- Silicon detectors since early 1990s, very good position resolution, good tracking detectors
- HL-LHC radiation scenario is challenging: Sensor developments for HL-LHC detector upgrades (~2024) are in the transition from R&D to prototyping
- TCAD simulations is a useful tool to understand device behaviour in irradiated environments → tune models and simulation parameters
- DU participated actively in tracker HPK campaign
- DU Jointly with other Indian Institutes in CMS, is planning to participate in the Phase-II Tracker Upgrade
- DU is involved in development of AC coupled Si sensors in India
- New detector technologies are under exploration
- Silicon sensor development will stay exciting! Stay tuned

Acknowledments & Litreture

- Some material taken from the following presentations & sources
  - Michael Moll, CERN, Charged Particle Tracking in High Energy Physics (ESI 2013)
  - Rainer Wallny, UCLA, Silicon Detector Workshop at UCSB May 11th, 2006
  - M. Krammer, Silicon Detectors, XI ICFA School on Instrumentation
  - Frank Hartman, Silicon Detectors
  - Alexander Dierlamm, Silicon Sensors for HEP Experiments, DAE-BRNS-HEP Symposium 2016
  - Endcap Calorimeter: Status Report, CMS Week 2016, TIFR, Mumbai
  - J. Zhang, PhD, DESY, 2013

- Literature: Further Reading
  - Frank Hartman, Evolution of Silicon Sensor technology in particle physics, Springer
  - G.Lutz, Semiconductor Radiation Detectors, Springer
  - H.Spieler, Semiconductor Detector Systems, Oxford University Press
  - G. F. Knoll, Radiation Detection and Measurement, John Wiley and Sons
  - S. M.Sze, Physics of Semiconductor Devices, Wiley-Interscience


THANK YOU FOR YOUR ATTENTION
ANY QUESTIONS?
memegenerator.net

Backup

CMS High Granularity Calorimeter

- $600 m^2$ (!) of silicon, 6M channels
- hexagonal pad detectors on 8” wafers ($0.5/1 cm^2$ individual pad size)
- tiny space for integration
- $F < 1 \times 10^{16} neq/cm^2$ and MIP sensitive ! (large capacitance ~ 40pF!)

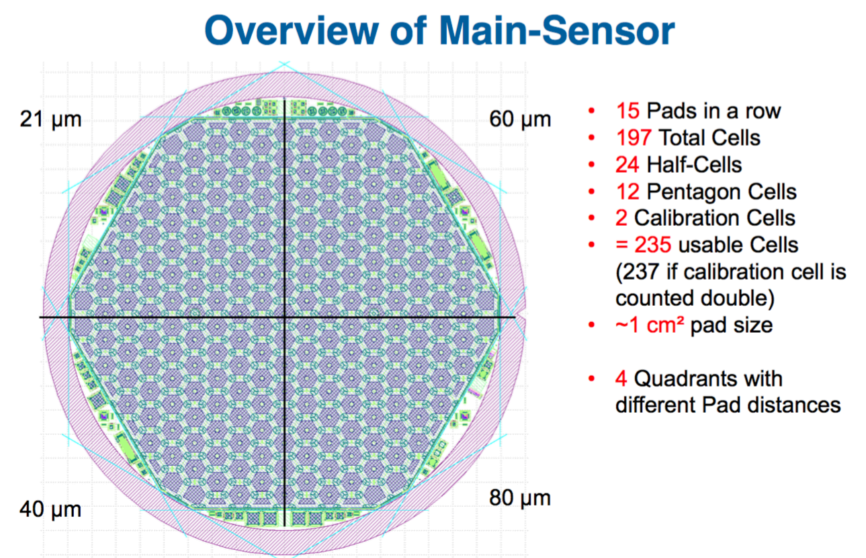

Overview of Main-Sensor

- 15 Pads in a row
- 197 Total Cells
- 24 Half-Cells
- 12 Pentagon Cells
- 2 Calibration Cells
- = 235 usable Cells (237 if calibration cell is counted double)
- ~1 cm^2 pad size
- 4 Quadrants with different Pad distances

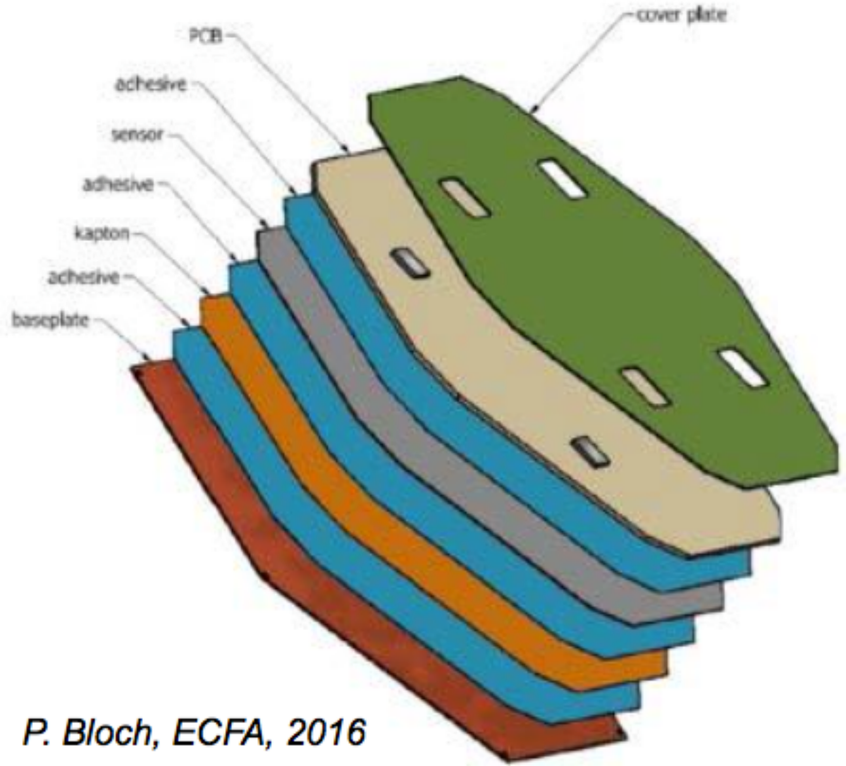

P. Bloch, ECFA, 2016

Structures in SILVACO

(1) Pad Diode

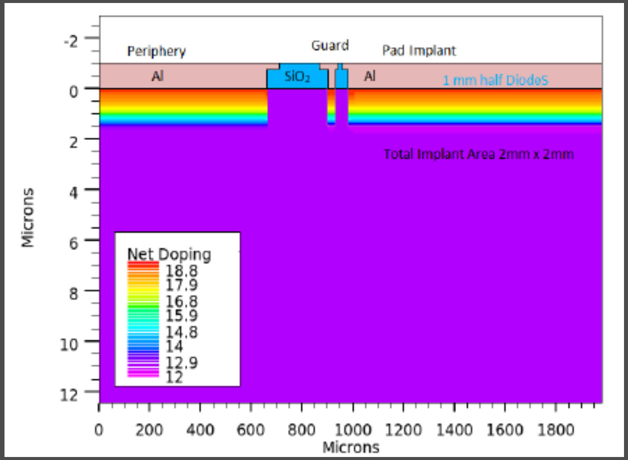

(2) Strip Detector

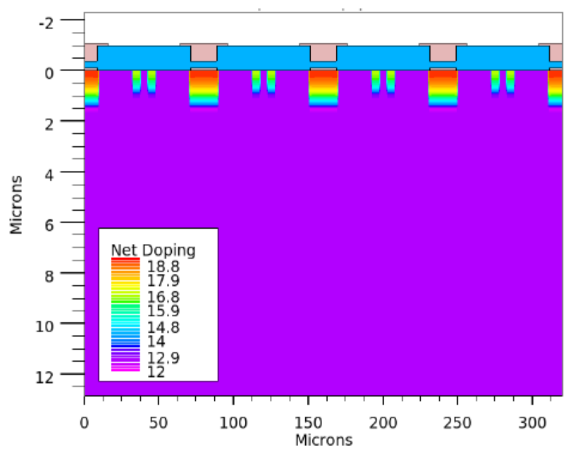

(3) Low Gain Avalanche Detector

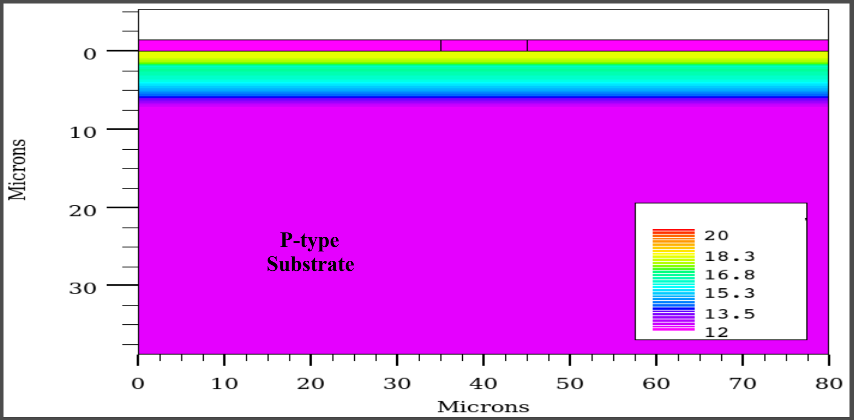

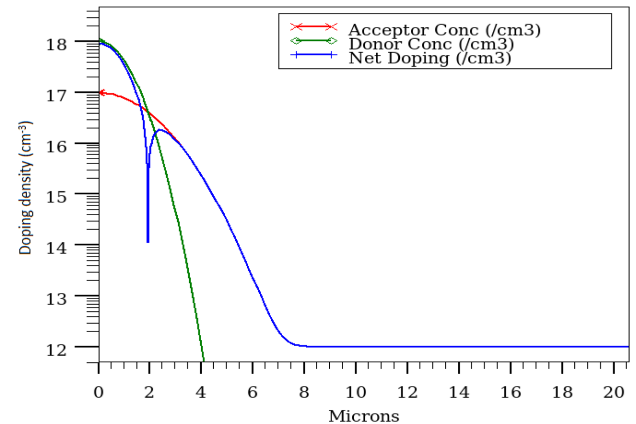

Pad Diode - IV

Detector is reverse dc biased. → Leakage current is measured (in dark).
Importance: Leakage Current value is a measure of NOISE at a particular voltage.
Critical at high fluence because SNR goes down.

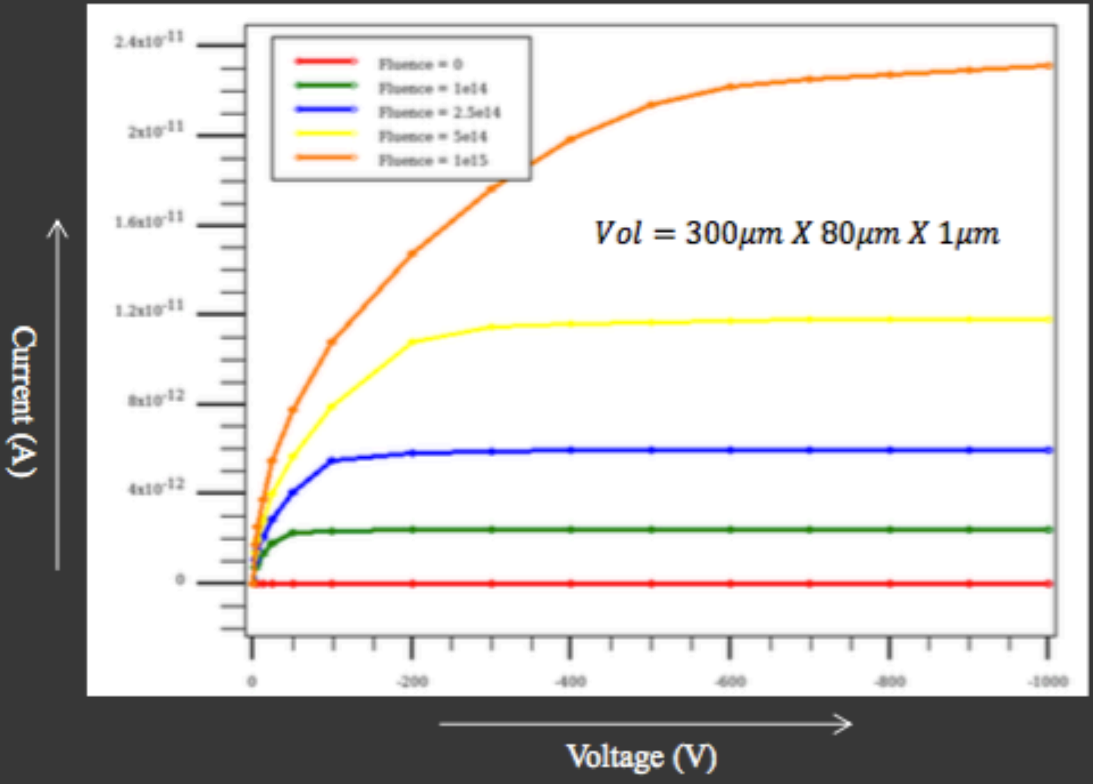

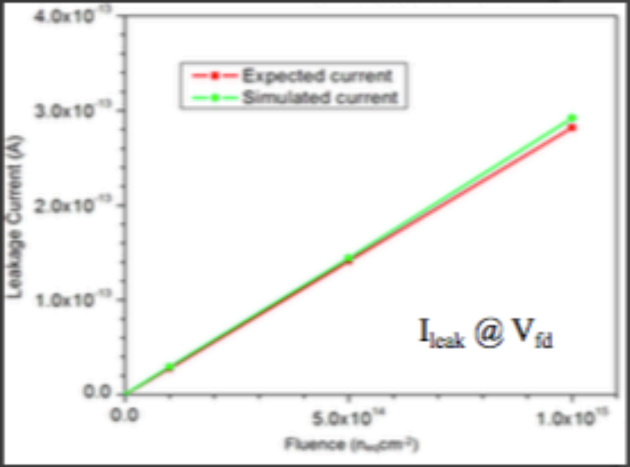

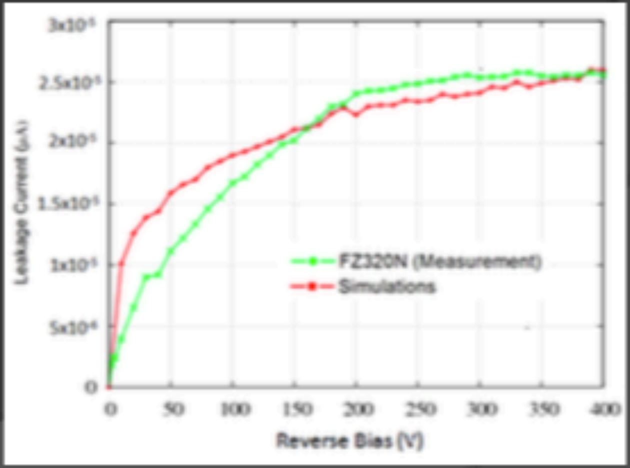

$$\Delta I = I_{irradiated} - I_{non-irradiated} = \alpha.\varphi.Vol$$
$$\alpha(253K) = 8.8\ X\ 10^{-19} A/cm$$

* CMS Detector Note. Simulation of Silicon Devices for the CMS Phase II Tracker Upgrade. CMS DN-2014/016.

Pad Diode - $C^{-2}V$

Detector is reverse dc biased & a small amplitude ac signal is provided at a frequency of 1kHz.
→ Impedance is measured.
Importance: Detector operation voltage is chosen 1.5 times of the full depletion voltage.

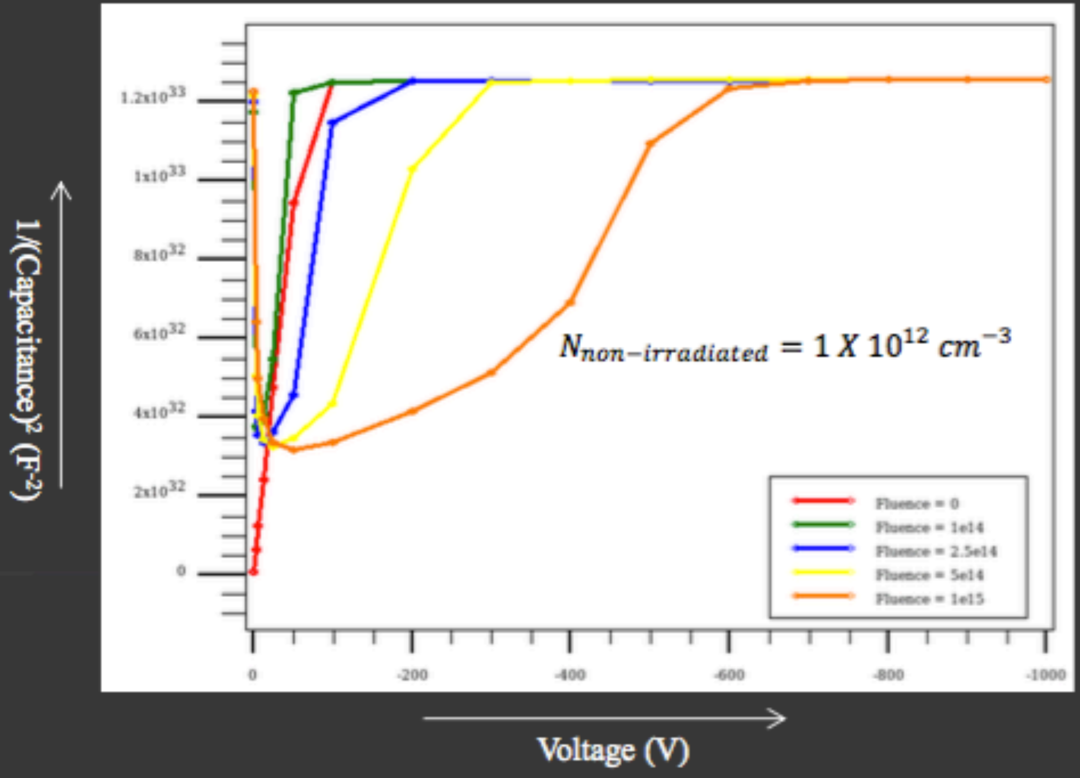

$$V_{fd} = \frac{ed^2}{2\epsilon} N_{eff}$$

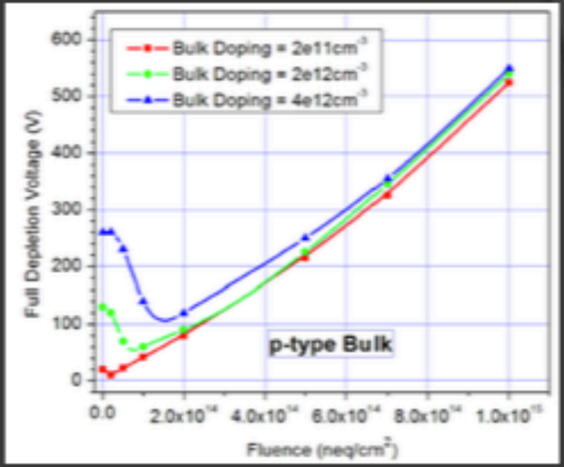

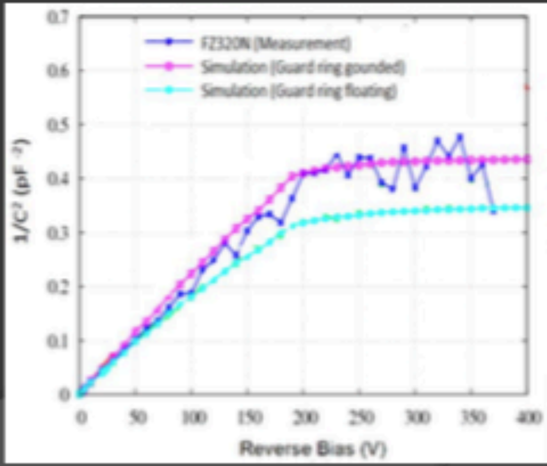

* CMS Detector Note. Simulation of Silicon Devices for the CMS Phase II Tracker Upgrade. CMS DN-2014/016.

Pad Diode - Transient Current Technique

Detector is reverse dc biased & an Infrared laser is shone from top or bottom. → Transient voltage is measured as a function of time.

Importance: Detector charge collection profile with voltage & fluence.

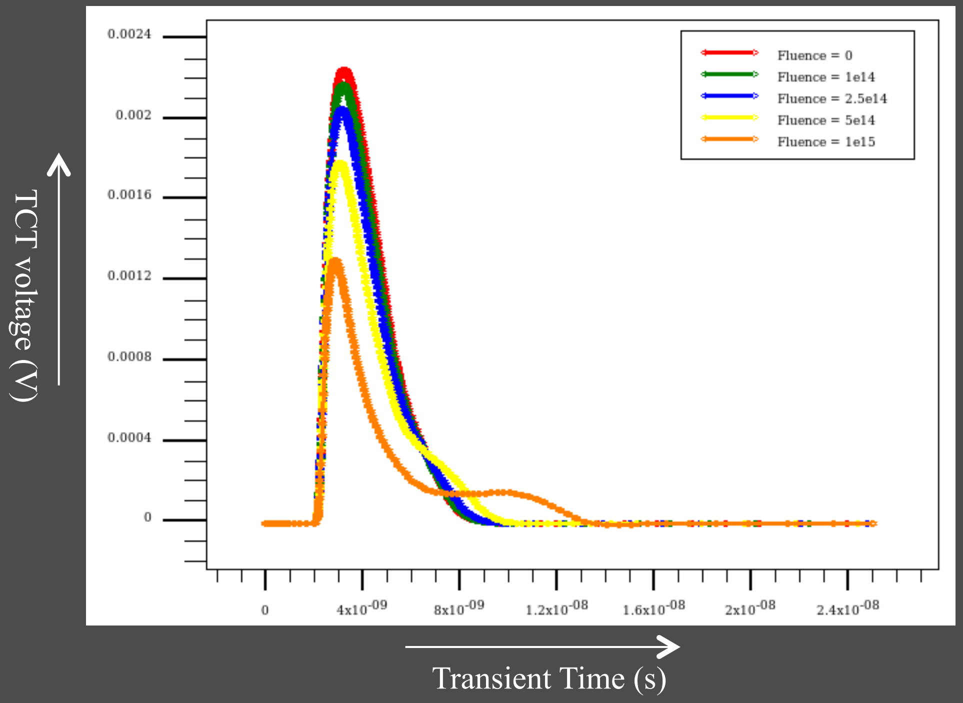

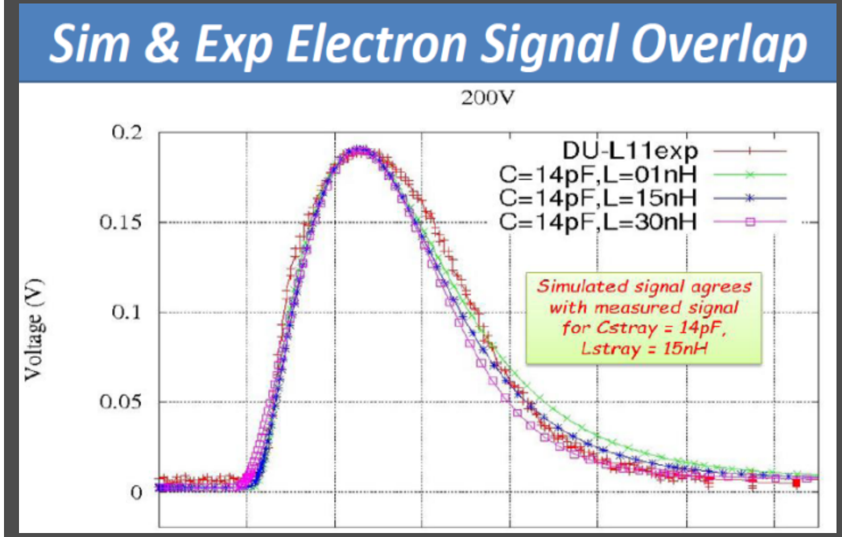

CC=area under IR laser TCT curve

* R. Dalal et al., PoS (Vertex2014)..

* G. Jain. Workshop on Contemporary Trends in High-Energy Physics and Experimentation. Panjab University. March 2014.

Simulated Result: Irradiated

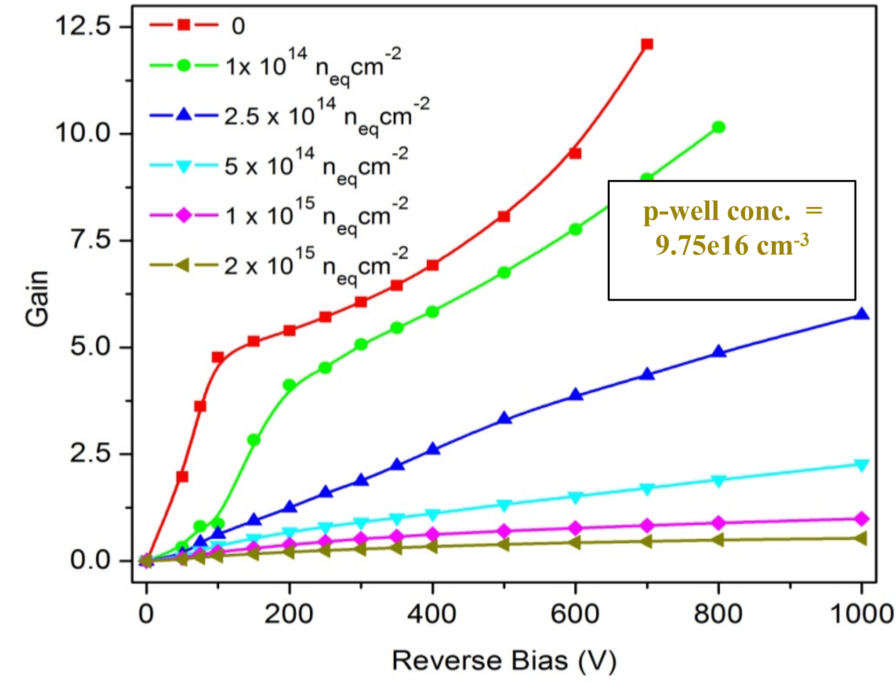

p-well conc. = 9.75e16 cm^{-3}

Peak E.field

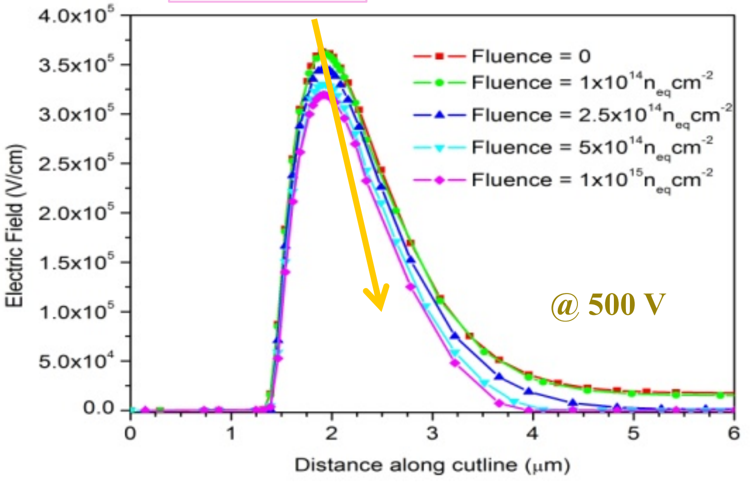

Bulk E.field

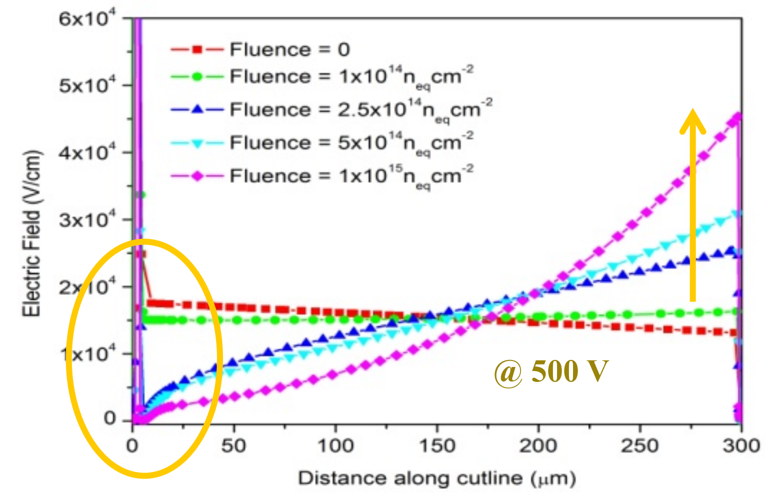

LGAD gain decreases with increase in fluence!

Because: 1. Peak e.field & its width decreases with fluence. E.field grows at backside of detector.
2. E.field just below the p-well region drops to very low value. Inefficient charge collection.

* R. Dalal, G. Jain, A. Bhardwaj, K. Ranjan. TCAD simulation of Low Gain Avalanche Detectors. NIM A. Manuscript accepted.

Radiation induced bulk defects relevant for detector operation

Electrical properties

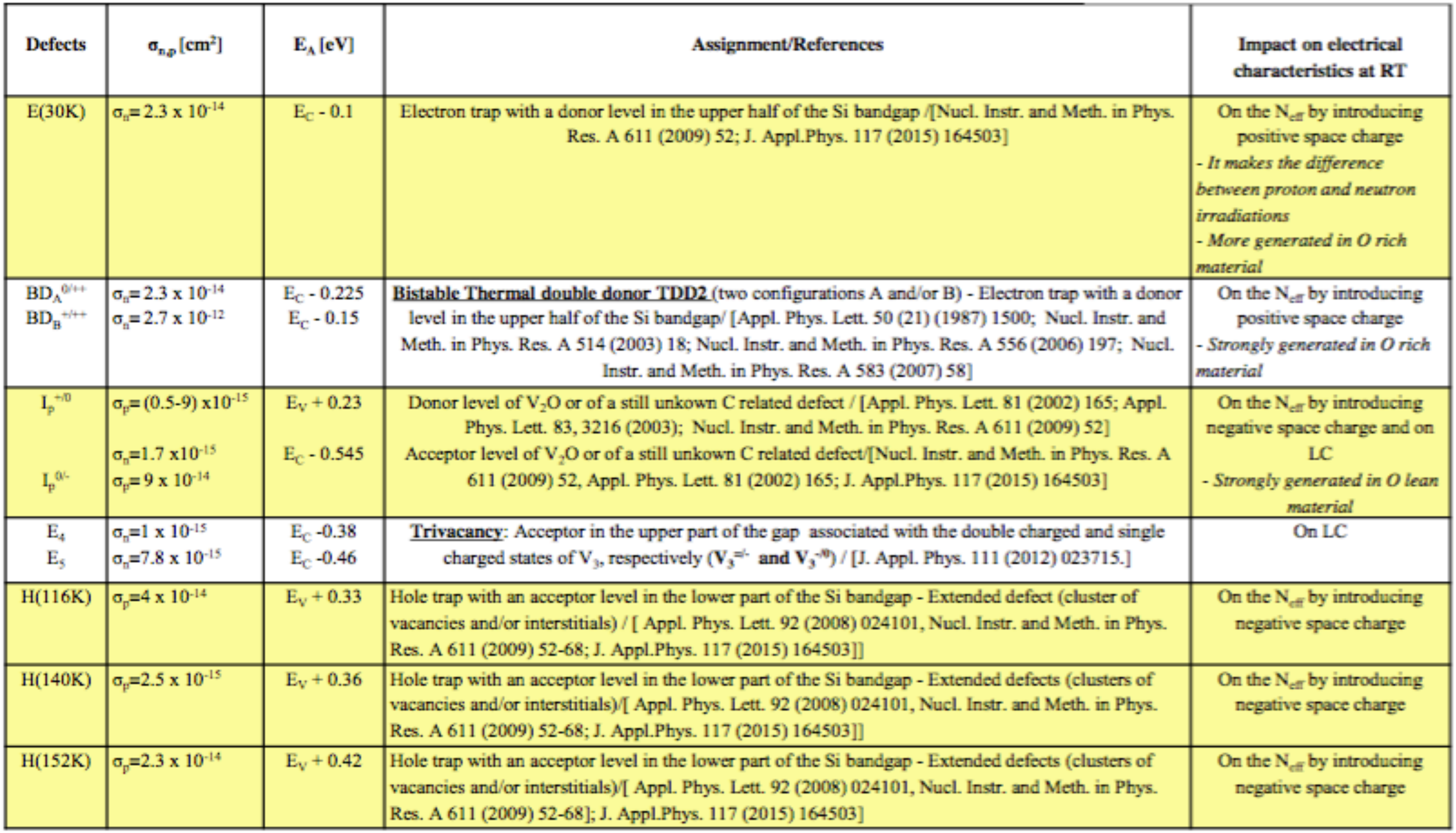

Defects	$\sigma_{n,p}$ [cm²]	E_A [eV]	Assignment/References	Impact on electrical characteristics at RT
E(30K)	σ_n= 2.3 x 10^{-14}	E_C - 0.1	Electron trap with a donor level in the upper half of the Si bandgap /[Nucl. Instr. and Meth. in Phys. Res. A 611 (2009) 52; J. Appl.Phys. 117 (2015) 164503]	On the N_{eff} by introducing positive space charge *- It makes the difference between proton and neutron irradiations* *- More generated in O rich material*
$BD_A^{0/++}$ $BD_B^{+/++}$	σ_n= 2.3 x 10^{-14} σ_n= 2.7 x 10^{-12}	E_C - 0.225 E_C - 0.15	**Bistable Thermal double donor TDD2** (two configurations A and/or B) - Electron trap with a donor level in the upper half of the Si bandgap/ [Appl. Phys. Lett. 50 (21) (1987) 1500; Nucl. Instr. and Meth. in Phys. Res. A 514 (2003) 18; Nucl. Instr. and Meth. in Phys. Res. A 556 (2006) 197; Nucl. Instr. and Meth. in Phys. Res. A 583 (2007) 58]	On the N_{eff} by introducing positive space charge *- Strongly generated in O rich material*
$I_p^{+/0}$ $I_p^{0/-}$	σ_p= (0.5-9) x10^{-15} σ_n=1.7 x10^{-15} σ_p= 9 x 10^{-14}	E_V + 0.23 E_C - 0.545	Donor level of V_2O or of a still unkown C related defect / [Appl. Phys. Lett. 81 (2002) 165; Appl. Phys. Lett. 83, 3216 (2003); Nucl. Instr. and Meth. in Phys. Res. A 611 (2009) 52] Acceptor level of V_2O or of a still unkown C related defect/[Nucl. Instr. and Meth. in Phys. Res. A 611 (2009) 52, Appl. Phys. Lett. 81 (2002) 165; J. Appl.Phys. 117 (2015) 164503]	On the N_{eff} by introducing negative space charge and on LC *- Strongly generated in O lean material*
E_4 E_5	σ_n=1 x 10^{-15} σ_n=7.8 x 10^{-15}	E_C -0.38 E_C -0.46	**Trivacancy**: Acceptor in the upper part of the gap associated with the double charged and single charged states of V_3, respectively (**$V_3^{=/-}$ and $V_3^{-/0}$**) / [J. Appl. Phys. 111 (2012) 023715.]	On LC
H(116K)	σ_p=4 x 10^{-14}	E_V + 0.33	Hole trap with an acceptor level in the lower part of the Si bandgap - Extended defect (cluster of vacancies and/or interstitials) / [Appl. Phys. Lett. 92 (2008) 024101, Nucl. Instr. and Meth. in Phys. Res. A 611 (2009) 52-68; J. Appl.Phys. 117 (2015) 164503]]	On the N_{eff} by introducing negative space charge
H(140K)	σ_p=2.5 x 10^{-15}	E_V + 0.36	Hole trap with an acceptor level in the lower part of the Si bandgap - Extended defects (clusters of vacancies and/or interstitials)/[Appl. Phys. Lett. 92 (2008) 024101, Nucl. Instr. and Meth. in Phys. Res. A 611 (2009) 52-68; J. Appl.Phys. 117 (2015) 164503]]	On the N_{eff} by introducing negative space charge
H(152K)	σ_p=2.3 x 10^{-14}	E_V + 0.42	Hole trap with an acceptor level in the lower part of the Si bandgap - Extended defects (clusters of vacancies and/or interstitials)/[Appl. Phys. Lett. 92 (2008) 024101, Nucl. Instr. and Meth. in Phys. Res. A 611 (2009) 52-68]; J. Appl.Phys. 117 (2015) 164503]	On the N_{eff} by introducing negative space charge

Inter-pixel Resistance & Max. E.Field

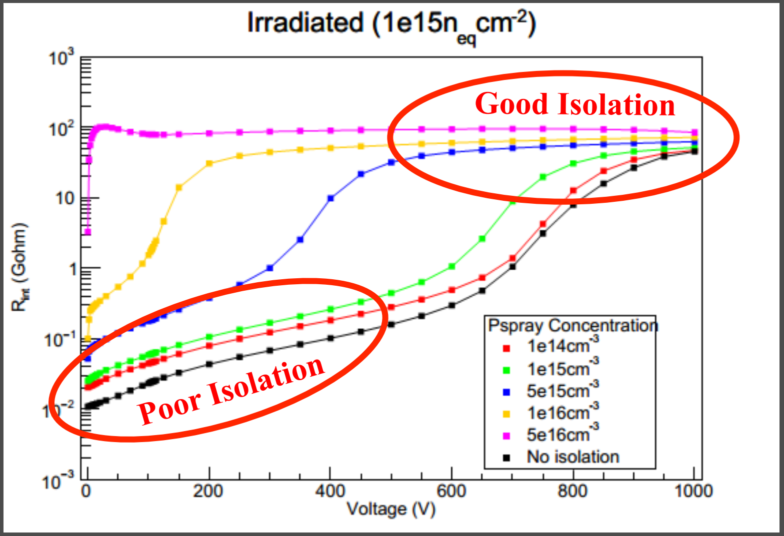

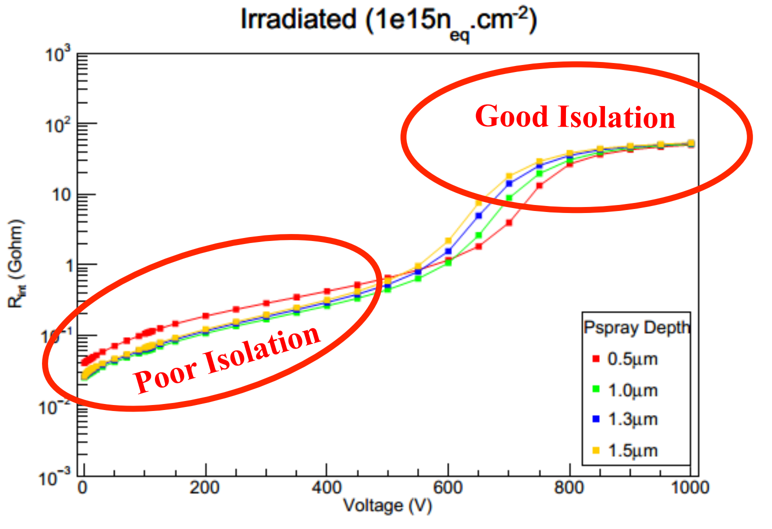

A higher concentration & a deeper pspray/pstop provides good isolation. But, this also leads to a rise in the electric field!

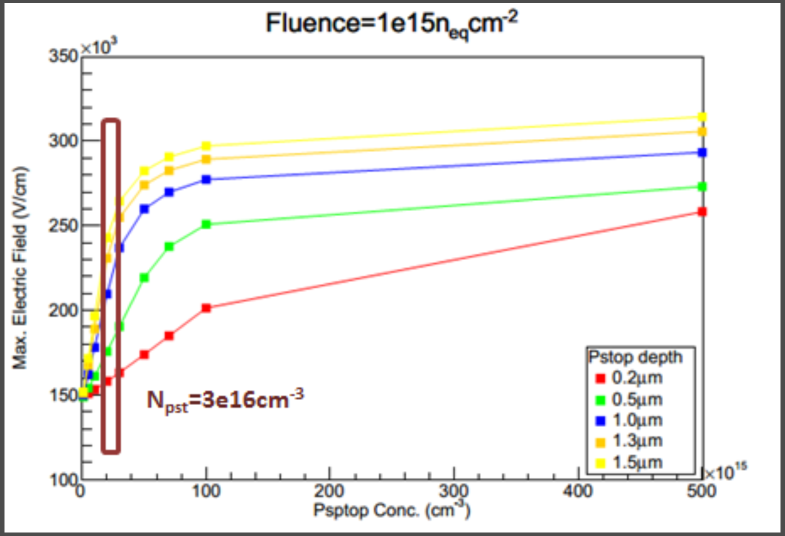

Therefore, an optimized concentration & depth of the isolation structure has to be chosen.

TCAD Simulations: Models & Numerical Methods

Equations for unknowns (*n*, *p*, *ϕ*):

Poisson Equation

$$\nabla^2\varphi = -\frac{\rho}{\varepsilon}$$

$$\rho = p - n + N_D^+ - N_A^-$$

Current Density Equation

$$J_n = q\left(n\mu_n E + D_n\frac{\partial n}{\partial x}\right)$$

$$J_p = q\left(p\mu_p E - D_p\frac{\partial p}{\partial x}\right)$$

Continuity Equation

$$\frac{\partial n}{\partial t} = \frac{1}{q}\nabla . J_n - r_n + g_n$$

$$\frac{\partial p}{\partial t} = -\frac{1}{q}\nabla . J_p - r_p + g_p$$

These equations use one of these specified models.

- These equations are solved using one of the methods.
- Extraction & Calculation of quantities

Physical Models:

a) Mobility – Concentration dependent, parallel field dependent
b) Impact ionization – Selberherr, Van Overstraten, Grant’s, etc.
c) Generation & Recombination – Shockley Read Hall
d) Oxide physics – Fowler-Nordheim, Interface charge accumulation
e) Statistics – Boltzmann, Band Gap Narrowing
f) Tunnelling – Band-to-band, Trap-assisted

Numerical Methods:

a) Gummel
b) Newton
c) Block

Width & Pitch

HPK Campaign

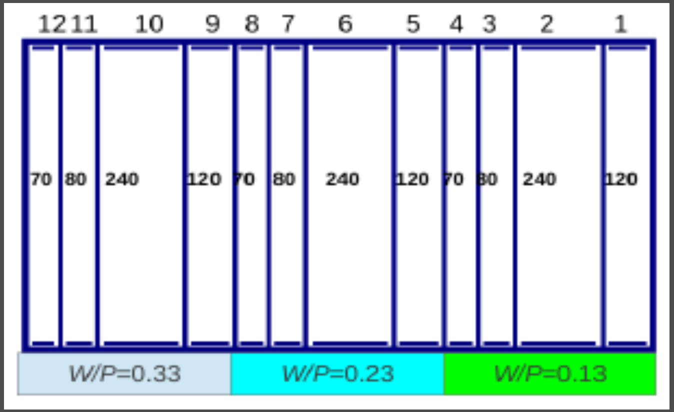

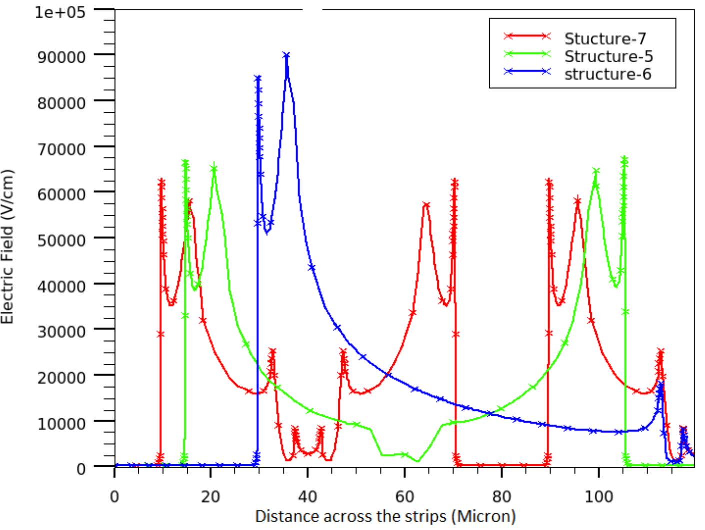

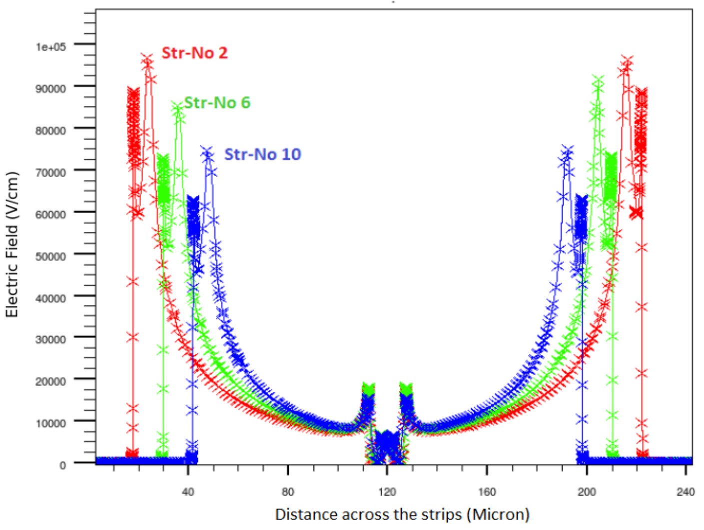

As the strip pitch increases, the electric field at the implant edge rises.

As the strip width increases, the electric field at the implant edge decreases.

* CMS Detector Note. Simulation of Silicon Devices for the CMS Phase II Tracker Upgrade. CMS DN-2014/016.

‘Simulation & Modeling’

A ‘simulation’ is an ‘imitation of reality’ !!

- How does it work?
  - The physical structure to be simulated
  - The choice of physical models
  - The numerical methods to solve the physical equations
  - The bias conditions for the electrical characteristics

Modeling: Comparison between Simulations & Measurements!!

- Choice of models & model parameters
- Tweaking of process & design parameters
- Optimization (multi-dimensional phase space) → Agreement of Macroscopic properties
- Fabrication of sensors with optimized design parameters

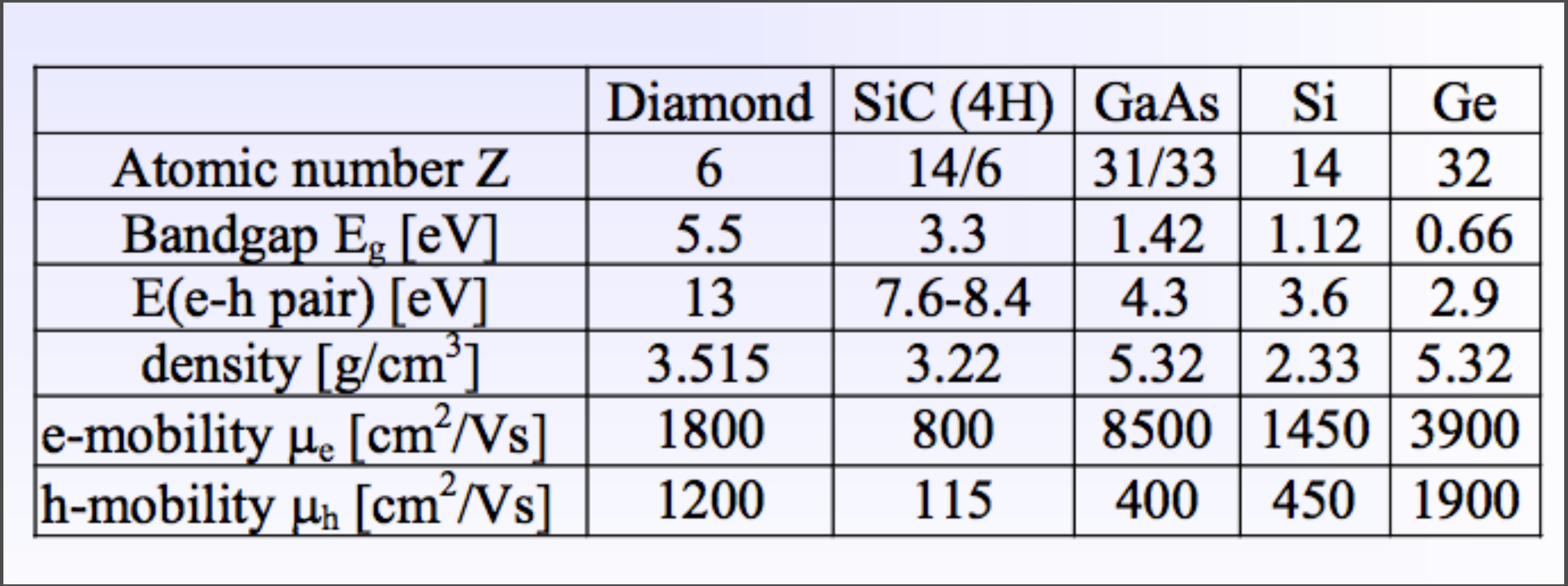

	Diamond	SiC (4H)	GaAs	Si	Ge
Atomic number Z	6	14/6	31/33	14	32
Bandgap E_g [eV]	5.5	3.3	1.42	1.12	0.66
E(e-h pair) [eV]	13	7.6-8.4	4.3	3.6	2.9
density [g/cm^3]	3.515	3.22	5.32	2.33	5.32
e-mobility μ_e [cm^2/Vs]	1800	800	8500	1450	3900
h-mobility μ_h [cm^2/Vs]	1200	115	400	450	1900

G. Kramberger, Radiation damage models, comparison and perfomance of TCAD simulation, Vertex 2016, Elba

Models of radiation damage in TCAD

EVL model
A single donor in bottom half of the bandgap and a single acceptor in the upper half of the bandgap

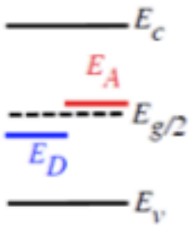

Perugia model
Three levels associated to donor CiOi, 1st acceptor to V_2 and 2nd acceptor to V_3

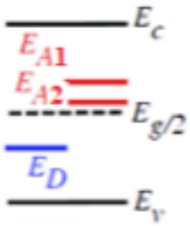

Model	E [eV]	g_{int} [cm^{1}]	σ_e[cm^{2}]	σ_h [cm^{2}]
EVL	Ev+0.48	6	1e-15	1e-15
Neutrons	Ec-0.525	3.7	1e-15	1e-15
Delphi	Ev+0.48	4	2e-15	2.6e-15
23 MeVp	Ec-0.51	3	2e-15	2e-15
KIT (Eber)	Ev+0.48	5.598 (-3.949e14)	2e-15	2.6e-15
23 MeVp	Ec-0.525	1.198 (+6.5434e13)	2e-15	2e-15
HIP	Ev+0.48	5.598 (-3.949e14)	1e-14	1e-14
23 MeVp	Ec-0.525	1.198 (+6.5434e13)	1e-14	1e-14
2 µm from surface only	Ec-0.40	14.417 (+3.168e16)	8e-15	2e-14
Hamburg (new)	Ev+0.48	1.51-2.75	8.37e-15	2.54e-15
	Ec-0.525	0.36-0.93	6.3e-15	8.37e-15

Model	E [eV]	g_{int} [cm^{1}]	σ_e[cm^{2}]	σ_h [cm^{2}]
Perugia	Ev+0.36	0.9	2.5e-13	2.5e-15
p-type	Ec-0.42	1.6	2e-15	2e-14
	Ec-0.46	0.9	5e-15	5e-14
Perugia	Ev+0.36	1.1	2e-18	1.2e-14
n-type	Ec-0.42	13	2.5-15	1.2e-14
	Ec-0.50	0.08	5e-15	3.5e-14
Peniccard	Ev+0.36	0.9	3.23e-13	3.23e-14
	Ec-0.42	1.613	9.5-15	9.5e-14
	Ec-0.46	0.9	5e-15	5e-14
Perugia new	Ev+0.36	0.9	3.23e-13	3.23e-14
(<7e15 cm^{-2})	Ec-0.42	1.6	1e-15	1e-14
	Ec-0.46	0.9	7e-15	7e-14

Title: Combined Bulk and Surface Radiation Damage Effects at Very High Fluences in Silicon Detectors: Measurements and TCAD Simulations
Authors: F. Moscatelli, et. al. Journal-ref: IEEE Transaction on Nuclear Science vol. 63, pp 2716-2723,2016, DOI: 10.1109/TNS.2016.2599560

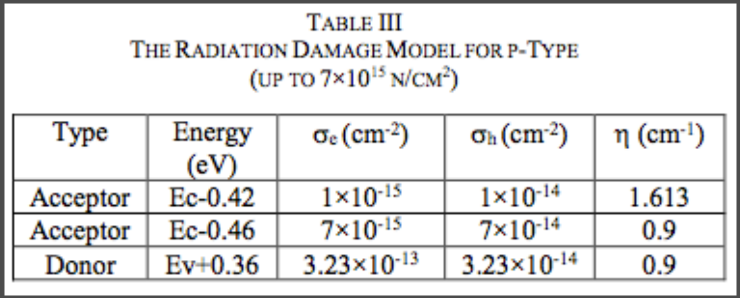

TABLE III
THE RADIATION DAMAGE MODEL FOR P-TYPE
(UP TO 7×10^{15} N/CM^2)

Type	Energy (eV)	σ_e (cm^{-2})	σ_h (cm^{-2})	η (cm^{-1})
Acceptor	Ec-0.42	1×10^{-15}	1×10^{-14}	1.613
Acceptor	Ec-0.46	7×10^{-15}	7×10^{-14}	0.9
Donor	Ev+0.36	3.23×10^{-13}	3.23×10^{-14}	0.9

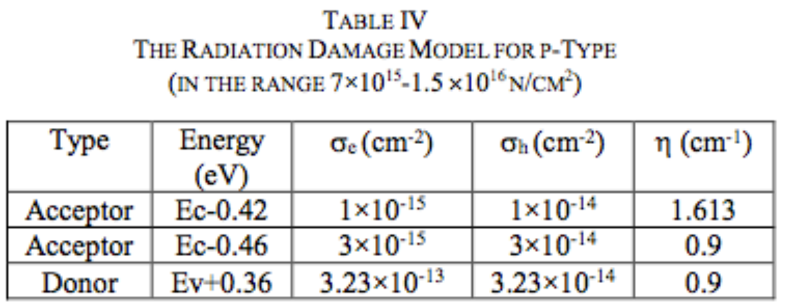

TABLE IV
THE RADIATION DAMAGE MODEL FOR P-TYPE
(IN THE RANGE 7×10^{15}-1.5×10^{16} N/CM^2)

Type	Energy (eV)	σ_e (cm^{-2})	σ_h (cm^{-2})	η (cm^{-1})
Acceptor	Ec-0.42	1×10^{-15}	1×10^{-14}	1.613
Acceptor	Ec-0.46	3×10^{-15}	3×10^{-14}	0.9
Donor	Ev+0.36	3.23×10^{-13}	3.23×10^{-14}	0.9

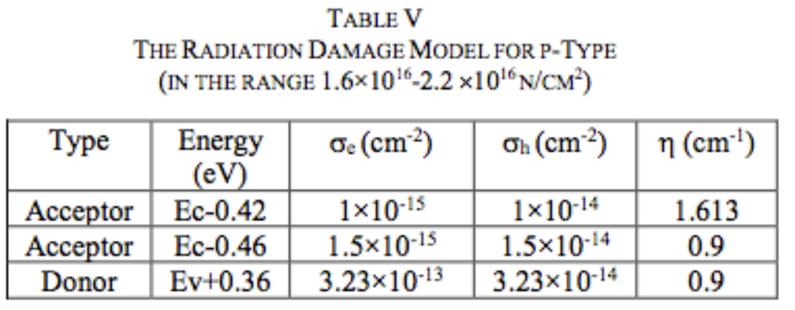

TABLE V
THE RADIATION DAMAGE MODEL FOR P-TYPE
(IN THE RANGE 1.6×10^{16}-2.2×10^{16} N/CM^2)

Type	Energy (eV)	σ_e (cm^{-2})	σ_h (cm^{-2})	η (cm^{-1})
Acceptor	Ec-0.42	1×10^{-15}	1×10^{-14}	1.613
Acceptor	Ec-0.46	1.5×10^{-15}	1.5×10^{-14}	0.9
Donor	Ev+0.36	3.23×10^{-13}	3.23×10^{-14}	0.9